COMPARISON OF HIGH-POWER DC-DC CONVERTER TOPOLOGIES FOR A NON-ROAD MOBILE MACHINERY APPLICATION

Lappeenranta–Lahti University of Technology LUT

Master's programme in Electrical Engineering, Master's thesis

2023

Tuomas Kiiski

Examiner(s): Professor Juha Pyrhönen

Anders Lindkvist, M.Sc. (Tech.)

ABSTRACT

Lappeenranta–Lahti University of Technology LUT

LUT School of Energy Systems

Electrical Engineering

Tuomas Kiiski

Comparison of high-power DC-DC converter topologies for a non-road mobile machinery application

Master's thesis

2023

92 pages, 25 figures and 6 tables

Examiner(s): Professor Juha Pyrhönen and Anders Lindkvist, M.Sc. (Tech.)

Keywords: NRMM, Earth-Moving Machinery, Mining industry, Electric vehicle, Trolley, Pantograph, DC-DC converter, Battery charging, Semiconductor switches

Interest for electrical mining machines is increasing all the time as environmental awareness is rising, emission legislation is becoming even tighter, and the development of power electronic technology has taken steps which enable it to be utilized efficiently in electrical drivelines of mobile machinery. However, technology still presents certain limitations especially for energy storages which reduce the usability of these machines that are run close to around the clock and could require high power even up to 1 MW for almost half of their drive cycle. As one solution to the problem, a pantograph solution is suggested with which the machine can connect to an external power source in a form of overhead catenary system during especially energy demanding parts of the drive cycle.

In this thesis a DC-DC converter part of such current supply arrangement is covered. Common components of DC-DC converters, a few typical step-down converter topologies are presented. Requirements for a DC-DC converter designed for mining machine and trolley application are defined and a market study is conducted to determine if such converters are available. Finally, the converters found are presented and compared against the set requirements and each other to determine which one is the most suitable for the intended use.

As a result, five different converter solutions presenting both IGBT and wide bandgap technology from different manufacturers are found and presented and three most promising ones of these are selected into the comparison. Comparison shows that each solution fulfils the basic requirements set but individual differences make one of the presented solutions more appealing than others.

TIIVISTELMÄ

Lappeenrannan–Lahden teknillinen yliopisto LUT

Energiajärjestelmät/LUT

Sähkötekniikka

Tuomas Kiiski

Liikkuviin työkoneisiin tarkoitettujen suuritehoisten DC-DC-konvertteritopologioiden vertailu

Sähkötekniikan diplomityö

2023

92 sivua, 25 kuvaa ja 6 taulukkoa

Tarkastaja(t): Professori Juha Pyrhönen ja Anders Lindkvist, M. Sc. (Tek)

Avainsanat: Liikkuvat työkoneet, Maansiirtokone, Kaivosteollisuus, Sähköiset ajoneuvot, Pantografi, DC-DC konvertteri, Akun lataaminen, Puolijohdekytkimet

Kiinnostus sähköisiä kaivoskoneita kohtaan on jatkuvasti kasvussa ympäristötietoisuuden kasvaessa, päästörajoitusten yhä tiukentuessa ja tehoelektroniikan otettua askeleita, jotka mahdollistavat sen käyttämisen liikkuvien työkoneiden sähköisissä voimalinjoissa. Markkinoilla oleva tekniikka kuitenkin asettaa yhä tiettyjä rajoituksia etenkin energian varastointiin liittyen, mikä pienentää näiden suurta tehoa pitkiä aikoja vaativien koneiden käytettävyyttä oleellisesti. Yhtenä ratkaisuna tähän ongelmaan on ehdotettu virroitinratkaisua (pantografi), jonka avulla kone voi kytkeytyä kaivoksen kattoon kiinnitettyjen ajolankojen muodossa olevaan ulkoiseen teholähteeseen suurta energiaa vaativien ajosyklin vaiheiden aikana.

Tässä diplomityössä käsitellään ylläkuvatun kaltaiseen virransyöttöjärjestelmään kuuluvaa DC-DC-konvertteria. DC-DC-konvertterien yleiset komponentit sekä muutama yleinen step-down -konvertteritopologia esitellään. Työssä asetetaan myös vaatimukset kaivoskoneeseen tarkoitetulle DC-DC-konvertterille, jonka jälkeen suoritetaan markkinakatsaus, jossa selvitetään, onko kyseiseen käyttöön soveltuvia konverttereita saatavana. Lopuksi löydettyjä konvertterit esitellään ja niiden ominaisuuksia verrataan asetettuihin vaatimuksiin sekä toisiinsa sopivimman konvertteriratkaisun löytämiseksi.

Markkinakatsauksen lopputuloksena löydetään ja esitellään viisi eri konvertteriratkaisua eri valmistajilta, joista kolme parhaiten sopivaa valitaan vertailuun. Vertailu osoittaa, että kaikki kolme konvertteriratkaisua täyttävät asetetut perusvaatimukset, mutta ratkaisuiden yksilölliset erot saavat yhden ratkaisun vaikuttamaan muita houkuttelevammalta.

ACKNOWLEDGEMENTS

I thank Epiroc for allowing me to write my thesis about this interesting and important subject for them and especially my instructor Mr. Anders Lindkvist for sharing me his in-depth knowledge about the mining industry. I thank also professor Juha Pyrhönen for his valuable advice and comments received during the writing process.

Finally, I want to thank my family and friends for the encouragement and support they have provided during this journey.

In Turku

4.4.2023

Tuomas Kiiski

SYMBOLS AND ABBREVIATIONS

Roman characters

B	Flux density	[T]
D	Duty cycle	
f	Frequency	[Hz]
H	Magnetic field strength	[A/s]
h	Conductor thickness	[m]
I	Current	[A]
l	Length	[m]
m	Mass	[kg]
n	Turns ratio	
P	Power	[W]
Q	Charge	[C]
R	Resistance	[Ω]
t	Time	[s]
T	Period	[s]
T	Temperature	[°C]
U	Voltage	[V]
V	Volume	[m³, l]

Greek characters

α	Angle	[°]
δ	Penetration depth	[m]
η	Efficiency	[%]
μ	Permeability	[H/m]
ρ	Resistivity	[Ωm]

Subscripts

CE	Collector-to-Emitter
CO	Cut-Off
CON	Conducting
D	Drain
DC	Direct current
DS	Drain-to-Source
fi	Falling current
fu	Falling voltage
G	Gate
GD	Gate-to-Drain
GE	Gate-to-Emitter
GS	Gate-to-Source
IN	In
OUT	Out
ref	Reference
r	Resonant

ri	Rising current
ru	Rising voltage
SW	Switching
th	Threshold

Superscripts

-	Lightly doped
‘	Referred to transformer’s primary side

Abbreviations

AC	Alternating Current
AI	Analogue Input
AMSL	Above Mean Sea Level
AO	Analogue Output
B	Base
BJT	Bipolar Junction Transistor
C	Collector
CAN	Controller Area Network
CC	Constant Current
CCM	Continuous Conduction Mode
CV	Constant Voltage
D	Drain
DC	Direct Current
DI	Digital Input

DO	Digital Output
DPS	Dual-phase-shift
E	Emitter
EMF	Electromotive Force
EMI	Electromagnetic Interference
EPS	Extended-Phase-Shift
ESL	Equivalent Series Inductance
ESR	Equivalent Series Resistance
ESS	Energy Storage System
EV	Electric Vehicle
FEM	Finite Element Method
FM	Frequency Modulation
FWD	Free-Wheeling Diode
G	Gate
ICE	Internal Combustion Engine
IGBT	Insulated-Gate Bipolar Transistor
IP	Ingress Protection
kbps	Kilobits per Second
Li-Ion	Lithium-Ion
LPF	Low-pass Filter
LV	Low Voltage
MOSFET	Metal-Oxide-Semiconductor Field-Effect Transistor
MTBF	Mean Time Between Failures
NA	Not Announced

NRMM	Non-Road Mobile Machinery
NMC	Lithium-Nickel-Manganese-Cobalt-Oxide
NMOS	N-Channel MOSFET
NRE	Non-recurring Engineering
OCL	Overhead Catenary Line
OCS	Overhead Catenary System
PCB	Printed Circuit Board
PLC	Programmable Logic Controller
PMOS	P-Channel MOSFET
Q	Quarter
S	Source
SIL	Safety Integrity Level
SoC	State of Charge
SPS	Single-phase-shift
TPS	Triple-phase-shift
VCA	Voltage Class A
VCB	Voltage Class B
WBG	Wide-Bandgap
ZCS	Zero Current Switching
ZVS	Zero Voltage Switching

Table of contents

1 Introduction

One of the biggest global issues current and coming generations have to face is the climate change which is caused by the greenhouse gas emissions heating our globe. News about glaciers melting at an ever-increasing pace and more frequent wildfires all around the world have become part of our everyday news feed. As the climate change is a global problem which affects everyone all around the world, many countries have agreed to take actions for example by means of changing legislation and taxation to support the change of moving from fossil fuel-based energy sources to renewable ones to reduce the carbon emissions.

Transportation is one of the most significant sources of carbon emissions globally by having a share of 17 % of all greenhouse gas emissions in 2019 (Climatewatch, 2023). Therefore, a lot of effort has been put on finding ways to reduce the carbon footprint of the heavy traffic, public transport, and private driving. Replacing internal combustion engines (ICE) and fuel tanks with electrical motors and battery packs and other non-fossil energy sources has been foreseen as one of the most promising ways of achieving this and for private cars the percentage of newly bought electric cars has been increasing for the last year rapidly.

For heavy transportation the change towards full electric trucks has not been as rapid mainly due to the lack of sufficient technology to store enough energy that the trucks require to operate as they need to cover longer daily driving distances than an average electric car owner. Concepts such as electric highways are being developed in multiple places all around the world, but they require more investigation and large investments to become popular.

Mining industry and mining vehicle manufacturers such as Epiroc are also shifting towards fossil-free energy sources in order to reduce their carbon footprint and find savings in the fuel costs. To give an idea about the scale of fuel consumption within a mining industry, according to an article written by Lindgren, Grauers, Ranngård & Mäki (2022), a single mine in Aitik, northern Sweden consumes 35000 m^3 diesel fuel yearly which corresponds to 0.4% of all petroleum-based energy sources used in the whole Sweden. Mining industry has found also other benefits from electrification of their loaders, trucks and drill rigs such as shown in Figure 1. In addition to saving the planet from greenhouse gases, especially in underground mines there is a huge advantage of having a zero-emission fleet as the exhaust gases of ICE’s do not need to be ventilated anymore and smaller amount of fresh air into the

mine is therefore required. Good air quality even in deep underground mines can then be achieved more easily while improving the quality of the working environment and saving energy. (Lindgren et al., 2022)

Figure 1. Some of Epiroc's full electric mining vehicles. (Epiroc, 2022, Epiroc Media Gallery)

Another reason for the mining companies to invest into the electrification of the machine fleet is the increase of productivity which it enables. Target for the mining companies is to maximise the amount of uphauled material whether it is ore or waste rock in a given time period while minimizing the operational costs. Electrical drivetrains allow high starting torque and higher top-speed in an uphill grade among other benefits when compared to diesel powered machines while reducing the operational and maintenance costs for example by eliminating the need for mechanical drivetrain components which require high maintenance especially in such challenging environment. (Mazumdar, Koellner & Moghe, 2010, p. 1158)

Full electrical vehicles also allow regenerative braking which allows vehicle to regenerate energy when travelling downhill by using the traction motors as generators. This reduces the wear of the mechanical brakes on the vehicle and allows some of the potential energy stored while travelling uphill to be stored back to the vehicle’s battery. Having an energy storage on board allows the energy to be utilized later on whereas with some diesel-electric hybrid trucks without one the energy would need to be dissipated in a brake resistor.

Epiroc for example has launched their “Smart and Green” series of fully electrical trucks in order to give a solution to these requirements coming from their customers. The reduced emissions have been taken into account from the beginning as the raw materials such as the steel from SSAB utilized in the production of the mining equipment is fossil-free and the battery packs produced by Northvolt are marketed as “the world’s greenest batteries”. Epiroc has committed into reducing their CO_{2e} emissions in half by 2030 and they are aiming to offer a complete range of emission free underground mining products by 2025. (Måård, 2022)

1.1 Problem setting

Diesel-electric hybrid mining vehicles have been around for decades already in open pit mines, but the development of semiconductor and battery technology has enabled the non-road moving machinery (NRMM) manufacturers such as Epiroc to start focusing on the development of their full electrical machine portfolio as well.

Epiroc’s MT42 Battery truck shown in Figure 2 is a medium sized model of their machine line meant for underground mines which can be used to haul ore and waste rock to the surface with its 42-ton loading capacity. It is based on the earlier model MT42 which utilizes traditional ICE to power the machine and is built on that same structure by replacing the mechanical drive train with an electrical one. It has two 200 kW traction motors in addition to one slightly smaller auxiliary motor for hydraulic system and a replaceable 470 kWh battery pack.

Figure 2. Minetruck MT42 Battery. (Epiroc, 2022, Epiroc Media Gallery)

MT42 Battery has been in production now for a few years and even though their customers have been extremely happy with it, they find that the battery could offer longer operating hours. Depending on the drive cycle the battery delivers energy for a few hours before it needs to be replaced with a freshly charged one. Changing the battery takes about 10 minutes and those charging stations are typically mined inside the tunnel systems of the mine. Even though this operation seems to be fast, the mining companies find that during the 16-hour daily operating time the time that goes into changing the batteries could be used more productively and therefore they have thrown a challenge to Epiroc which they have taken – Improve the operating time of the machine.

Underground mining vehicles need to be small, compact, and agile when compared to their surface counterparts to minimize the cross-section of the tunnels. There simply is no room to place a larger battery pack on the machine and the efficiency of the drivetrain could be improved only slightly so other effective solutions need to be thought of. One such approach is to utilize so-called trolley system that Cruzat & Valenzuela (2018) define as a configuration that allows the machine to draw power from the electric grid of the mine to power its traction motors. In a trolley system connection to the mine's electricity distribution system is established by using so-called trolley lines instead of having an onboard cable reel such as some tethered machines, typically drill rigs, utilize. According to press release (Andersson, 2021) published also in several industry publications Epiroc, Boliden and ABB have a joint project which aims to build this kind of trolley system in Boliden's Kristineberg mine. In practice, substations supplied from medium voltage grid and an overhead catenary line (OCL) are built into the Kristineberg mine. The substations transform the mains voltage into low voltage and rectify it before feeding it to the respective OCL segments that are built on the ceiling of the mine tunnel and hang over the load hauling ramp. A pantograph is added on the machine to allow it to contact this external power source in a similar way as in electric trains, trams and trucks on electrical highways that are also currently under development. Trolley assisted trucks have been around for decades in open pit mines and they have proven to increase the productivity remarkably due to the increased upgrade speed, reduced travel time and fuel savings while improving the sustainability of the mining operations. (Cruzat et al., 2018, p. 3971-3972; Lindgren et al, 2022, p. 1–19; Swallow, 2021).

1.2 Objectives and delimitations

Such modification presented in the earlier chapter however requires some large additional parts to the already tightly packed machine. The machine needs to have a pantograph to allow connection to the OCL and the voltage of the overhead catenary system (OCS) needs to be converted to suit the voltage of the vehicle's battery and drivetrain's DC-link voltage. Because the OCL voltage needs to be high in order to minimize the distribution losses in the system, the voltage of the OCL is higher than the voltage of the machine's DC-link. Therefore, the focus is on topologies that provide step-down functionality or both step-down and step-up functionality. Converters providing only step-up functionality are out of interest of this thesis.

Project parties have decided to realize the OCS by using direct current (DC) low voltage (LV) distribution that is isolated from the earth to mitigate some safety issues. DC-DC conversion is therefore required but it is also beneficial over AC-DC conversion since it reduces the size of the vehicle mounted converter. One of the largest single components required in such AC-DC converter is the transformer which requires a lot of volume and could have mass close to one ton when operated at the grid frequency.

Epiroc's truck portfolio intended for underground mining operation consists of multiple different sized trucks of which loading capacity varies from 20 tons to 65 tons. All of these truck models have not yet been released as an electrical version but those are also under development. Therefore, the study should take different power requirements of the whole portfolio into account so that it is possible to apply similar current supply solution to the whole machine range in the future. This means that the required output power of the converter varies roughly from 400 kW up to 1 MW to cover the power requirement for traction motors, auxiliary systems and charging of the battery. Similar current supply solution could be installed also to loaders that often drive same route back and forth but, in this thesis, only application for trucks is considered.

The focus of this thesis is to find out the best possible DC-DC converter topology and solution in terms of power density, efficiency, and suitability for this kind of high-powered NRMM application. This will be done by studying the structures of different converter topologies and solutions their key features to find the advantages and disadvantages of each system.

Thesis will also present the common components used in the converters and cover development in the field of semiconductor technology. Focus is on the traditional silicon (Si) based semiconductors such as insulated-gate bipolar transistors (IGBT) which have been the de facto component for high power switching applications for years and wide-bandgap (WBG) semiconductors such as silicon carbide (SiC) and gallium nitride (GaN) transistors which have taken huge leaps in development over the latest years and are to be on par with IGBTs soon while providing some additional advantages.

The thesis will not cover design or dimensioning of a converter or its components and describing operation principles of different converter topologies must be limited to trivial level as each of these topics covered in greater detail would be a thesis topic of its own. Design of the sub-station, OCS, current collector, input filter, machine driveline or any other part of the system and evaluating their performance and feasibility are interesting topics as well but out of the scope of this thesis.

1.3 Literature review

While this is not the first time trolley solutions like this are used in underground mining vehicles, only a very few attempts have been made earlier to implement such a design and even then, the approaches have been quite different relying on AC distribution systems. One example of this kind of approach known as “Kiruna truck” is presented for example in the study conducted by Paraszczak, Sedlund, Fytas & Laflamme (2014, p. 83–84). On open pit diesel electric hybrid trucks that are many times larger than their underground counterparts a similar kind of approach has been successfully implemented on multiple occasions but also these have relied on AC distribution networks and the approach has therefore been different. Therefore, DC-DC converter comparison directly for this application has not been either done or published before or at least such was not found.

Comparison of converters and converter topologies for other applications such as electric vehicle (EV) charging applications has been done earlier and their contents overlap to some degree as similar topologies can be used but the use cases typically differ both in terms of voltage and power levels. One good example of such a paper is a study conducted by He and Khaligh (2017, p. 147 – 156) in which they compare different kinds of isolating bidirectional DC-DC converters for EV charging system. The said study covers dual active bridge and

CLLC resonant converter circuits in their half-bridge and full-bridge topologies but does not cover simpler unidirectional topologies such as buck and fly-back converters. It also covers converters designed for voltages up to 500 V and power up to 1 kW, so the result and focus are slightly different. Another comparison of high-power DC-DC converters is done by Steigerwald, De Doncker & Kheraluwala (1996) in which four different soft switched converter topologies are compared against hard-switched pulse width modulation (PWM) controlled full-bridge converter, which acts as a baseline. Since their study is written almost 30 years ago and each of the proposed converters are realized using Si-based IGBTs, the concrete values are not comparable to today's WBG based converter designs. The study, however, gives a good insight for example on how the efficiencies and the masses of the magnetic components compare between the different topologies and example designs that are similar in power.

Lindgren et al. (2022) have simulated the feasibility of trolley-assisted full electric surface mining trucks against the diesel powered and trolley-assisted diesel-powered mining trucks from a viewpoint of operating costs with predetermined drive-cycles and battery dimensioning. Their study however does not cover the converter technology used in the trolley system at all therefore leaving room for study conducted in this thesis.

Koellner, Brown, Rodriguez, Pontt, Cortes & Miranda (2004) have also covered similar things while studying trolley-assisted diesel-powered mining trucks, but their focus has been on inverters and different operating modes among other things. Also being almost 20 years old study, a lot has happened in the field of semiconductor technology which has affected some of the statements they have made.

Mazumdar et al. (2010) have studied the interface issues of trolley assisted mining vehicles which are applicable for this project as well but affect mostly the input filter design which is not in focus of this thesis. Their study however sets some operational and environmental requirements which are quite well in line with the ones set for the Epiroc's machines.

1.4 Research questions and methods

Two research questions are set for which answers are presented in this thesis. The first research question is how much better power density can be achieved in a high-power DC-

DC converter by using wide bandgap components instead of traditional Si-components and second one is which one of the commercial solutions on the market suits the best the needs of the Epiroc.

The following research methods are used to conduct the study reported in this thesis. Research of semiconductor and converter technology theoretics is conducted by studying scientific articles and publications about these topics. The requirements for the converter are set based on the initial parameters of the system decided within the project, limitations set by the base machine, standardization, risk assessments and discussions with Epiroc employees that are working in the project and have knowledge of the existing base machines. The market study is conducted by searching suitable manufacturer candidates from the internet, contacting them, and having discussions with them to learn about what kind of solution they could offer. Finally, a side-by-side comparison of the most suitable solutions is made by breaking the solutions into smaller sections such as electrical or mechanical properties and going through each section one by one while comparing the solutions against the requirements and one another to determine which one is the most suitable.

2 DC-DC converters in general

This chapter gives an insight to the converter technology in general. The common components of DC-DC converters such as semiconductor switching components and discrete passive components are presented. The basic structure and operating principles of the semiconductor components as well as the recent progress in the development of WBG technology are covered and a brief insight into the discrete passive components used in high power converters is given focusing, especially, on the characteristics that are important in such an application. Finally, a few different common DC-DC converter topologies which are used to step down the voltage are presented to give an idea of the structure and operating principles of different topologies.

2.1 Semiconductor components

Different semiconductor components can be used in DC-DC converter topologies the most common ones being different kinds of transistors and diodes. Each of these serve their own purpose transistors being typically used as switches that and diodes as rectifiers or free-wheeling diodes. Generally, transistors are used in DC-DC converters as switches toggling the current on and off allowing the inductive and capacitive components of the converter to be charged and discharged on which the whole operation of the DC-DC converters is practically based on. The diodes have different purposes on different topologies and all topologies do not utilize them at all. Some converters such as buck converters utilize diode to determine the direction of the current flow when the semiconductor switch is toggled. Some isolated half-bridge and full-bridge converters on the other hand can utilize diodes on their secondary stage to rectify the AC of the intermediate stage back to DC. The simpler topologies have only a single transistor and a single diode whereas more complex converters can have typically up to eight switches.

A detailed description of physics behind the operating principle of semiconductor components is not included in this thesis but some of the key concepts are explained. Semiconductors are manufactured by doping a substrate such as pure Silicon wafer with small amounts of other elements from a different column of periodic table such as Boron,

Gallium, Phosphorous or Arsenic that either have larger or smaller amount of valence electrons than the substrate. Doping is done to release free charge carriers from the covalent bonds of different atoms have between them. Depending on the element used for doping the resulting semiconductor has either free holes (i.e., missing electrons) or extra electrons on its valence band and based on this, semiconductors can be divided into p- and n-type. A p-type semiconductor has free holes as its majority charge carrier and free electrons as minority charge carrier whereas n-type semiconductor has free electrons as its majority charge carrier and free holes as minority charge carrier. (Dimitrijev, 2012, p. 17)

According to Erickson & Maksimovic (2020, p. 79) one of the main challenges with power semiconductor is to achieve high break-down voltage while having low forward voltage drop and on-state resistance. Erickson et al. state that a high break-down voltage of a p-n junction requires a low doping concentration which then again results in a high on-state resistivity due to the low number of charge carriers. He then continues by explaining that in majority-carrier devices such as Metal-Oxide-Semiconductor Field-Effect Transistors (MOSFET) and Schottky diodes this dependency is inevitable. However, in minority-carrier devices such as bipolar junction transistors (BJT) and IGBTs a phenomenon called conductivity modulation results in a lower on-state resistance than in a comparable majority-carrier device. Because of the larger controlling charges required to turn on and turn off the minority-carrier devices the switching speed of these components is slower than the same of a comparable majority-carrier device. This explains the higher switching frequencies that can be achieved with MOSFETs when compared to IGBTs. However, using SiC as the base material when manufacturing a MOSFET offers, in practice, as good conduction properties as silicon IGBTs but at the same time much better switching properties than an IGBT. In principle, one could produce also an IGBT with SiC but manufacturing components from SiC is so difficult that there are quality problems even with the simple MOSFET construction and at the moment there are no SiC IGBTs available.

2.1.1 Diodes

A p-n junction is the most basic semiconductor structure, and it can be found from many components in different combinations. A single p-n junction forms also a diode. In general, diodes can block current flow when reverse voltage is applied but when high enough forward

voltage is applied over them, they start to conduct current exponentially. There are different kinds of diodes such as Zener and Schottky diodes in addition to traditional and power diodes but those are not considered in this thesis. A diode has two terminals, an anode and a cathode.

Power diodes are formed by doping either p or n side of the junction very lightly. This way the breakdown voltage of a diode can be increased effectively and in case of silicon-based diodes the breakdown voltage up to a few kV can be achieved. However, the low doped region increases the on-state resistance and forward voltage causing remarkable power losses over the diode. Therefore, doping is done in such way that only a portion of other side of p-n junction is lightly doped while the rest of the substrate is more heavily doped. The lightly doped layer is called as drift region. (Dimitrijev, 2012, p. 533–535)

Structure of power diode or a diffused-junction p-n diode is shown in Figure 3 where n^- is the drift layer and p and n are the heavily doped regions. According to Erickson et al. (2020) when reverse voltage is applied across the power diode the diode is in non-conducting state and the most of this voltage is across depletion region in the drift region. Then again, when forward voltage is applied across the diode holes are injected from p to n^- region after which they are recombined with free electrons of n region. These injected holes become minority charge carriers in n-region, and they reduce the apparent resistivity of the drift region. (Erickson et al., 2020, p. 83)

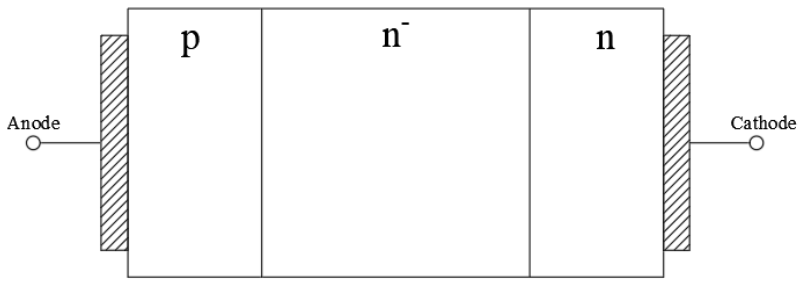

Figure 3. Power pn-diode structure.

According to Dimitrijev (2012), the drift region doping level and its length define the blocking voltage and the on-state resistance of the power diode. He concludes that the higher

the blocking voltage is also the higher the on-state resistance becomes. (Dimitrijev, 2012, p. 533–535)

2.1.2 MOSFETs

MOSFET is another semiconductor component commonly used as a switch in different kind of electronic circuits ranging from small battery powered devices to large high-power systems. MOSFETs have four terminals – gate (G), drain (D), source (S) and body (B) of which S and B are in most cases shorted together. MOSFETs are built out of two p-n junctions and there can be both p-channel (PMOS) and n-channel (NMOS) MOSFETs. In addition, MOSFETs can be divided into enhancement and depletion types based on if they are conducting while gate-to-source voltage U_{GS} is applied or not. However, depletion type MOSFETs are rather rarely used and therefore only enhancement type MOSFETs are considered in this thesis. Figure 4 presents the structure of NMOS in on-state. In Figure 4 metallized S and D terminals are shown at the top and bottom. Polysilicon G terminal is also shown on the top. Two p-n junctions are easily distinguishable from it also and so-called body diode structure similar to one of power diode is formed from the p-n^- junction. A similar lightly doped region can also be found from the power MOSFET as is in the power diode. (Erickson et al., 2020, p. 99-103; Dimitrijev, 2012, p. 296–300)

When no gate-to-source voltage U_{GS} is applied or when it is smaller than the threshold voltage U_{th}, MOSFET is in non-conducting off-state, the drain-to-source voltage $U_{DS} > 0$ and drain current $I_D = 0$. When high enough gate-to-source voltage $U_{GS} > U_{th}$ is applied conducting channels are formed under the G terminal on the p region between D and S terminals allowing drain current I_D to start flowing as shown in Figure 4. When the channel is formed it can be seen as a parasitic resistor which causes I_D flowing through the channel to increase linearly when U_{DS} is also increased making MOSFET an unideal switch. (Dimitrijev, 2012, p. 299)

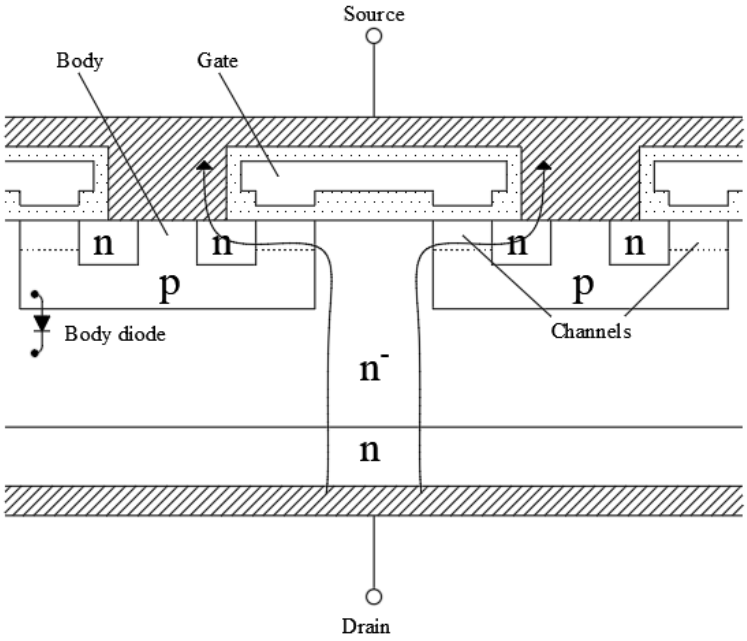

Figure 4. NMOS structure in on-state.

According to Erickson, the on-state resistance of a MOSFET is a sum of all the resistances there are in the device meaning resistances of drift region, the channel, S and D terminal contacts and so on. For power MOSFETs starting from roughly 700 V the drift region resistance is dominating the on-state resistance. (Erickson et al., 2020, p. 99–103)

2.1.3 IGBTs

IGBT is another semiconductor switch component which is used commonly especially in applications where high-power and voltage switching is required. The structure of IGBT is very similar to one of MOSFET the difference being the additional p region connected at the Collector (C) terminal as shown in Figure 5. Additional p region injects minority carriers into n^- region while the IGBT is forward biased and conducting causing conductivity modulation to reduce the on-state resistance of the n^- region. This allows even the high-voltage IGBTs rated for a few thousand volts to have a forward voltage drop of just two to four volts typically. Another difference is the naming of the terminals. Instead of Drain and Source that MOSFET has, the IGBTs terminals are called Emitter (E) and Collector (C) like in BJT but instead of Base (B) the IGBT has Gate (G) like a MOSFET. This is actually due to the IGBT being a cascade connection of a MOSFET and a PNP BJT as shown in Figure

5. The MOSFET is practically used to drive the BJT, which allows the IGBT to conduct high currents like a BJT without the need for continuously supplying base current to maintain the on state like a MOSFET. (Erickson et al., 2020, p. 115–119; Dimitrijev, 2012, p. 541)

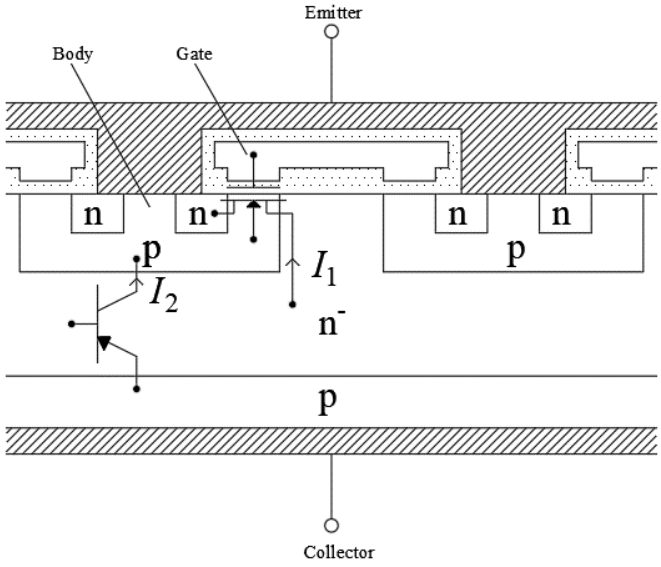

Figure 5. IGBT structure

Dimitrijev (2012) explains that while no gate-to-emitter voltage U_{GE} is applied to IGBT it is in off-state and its equivalent circuit could be described as a BJT of which base has been left unconnected resulting the IGBT to look like two back-to-back connected diodes. This results IGBT to have voltage blocking capacity to both forward and reverse voltages unlike power MOSFET which can only block forward voltages. This is a significant advantage or disadvantage depending on the application. When U_{GE} is increased to sufficient level exceeding I_{th} an inversion layer is formed which connects n^- layer, n regions and emitter terminal together. This allows major part of collector-to-emitter voltage U_{CE} to drop across the lower pn-junction making it forward biased and causing holes to be injected to n^- layer which carry most of the on-state current. Simultaneously apparent MOSFET supplies electrons to maintain the forward bias. (Dimitrijev, 2012, p. 541–542; Erickson et al., 2020, p. 115–119)

As Figure 5 shows, there are two different currents flowing in IGBT, I_1 flowing through MOSFET and I_2 flowing through BJT. According to Erickson, especially the turn-off switching time of an IGBT suffers greatly from the reduced voltage drop due to phenomenon

called current tailing. IGBT is switched off by removing gate charge from MOSFET by applying negative U_{GE} which causes it to stop conducting so that I_1 becomes zero quickly. BJT will however continue conducting current I_2 as long as there is minority charge in n^- layer and as only way to remove this charge is by natural recombination, a current tail proportional to minority charge is to be observed. This results in typical turn-off times of an IGBT to be in range of 0.5-5 µs whereas the same of a MOSFET is below 100 ns. (Erickson et al., 2020, p. 103–119)

2.1.4 Si versus WBG semiconductors

Silicon-based power semiconductors have dominated the market for well over the past half a century. Even though that technology has developed much during these years it is about to reach its theoretical peak performance what it comes to blocking voltage, operation temperature and conduction and switching characteristics and therefore the development is slowing down and eventually stopping. (Wang, Zhang & Jones, 2018, p. 1–12)

As Si technology has more or less reached its maximum potential the only way to further improve the characteristics of semiconductors to meet the tomorrow's requirements is to replace the Si technology with a different one. So called wide bandgap (WBG) technologies are being developed to overcome the Si technology in the power and radio frequency electronics. WBG technologies designed especially for power electronics include but are not limited to silicon carbide (SiC), gallium nitride (GaN), diamond and gallium (III) oxide (Ga_2O_3) technologies. However, SiC and GaN technologies are currently the two most mature and potential ones of these to challenge Si technology's market lead and therefore focus on this thesis will be on these WBG technologies. Both of these come in variety of different crystal structures or polytypes such as SiC-4H or GaN-2H which are considered to have the most interesting characteristics for power electronic applications. (Ballestín-Fuertes, Muñoz-Cruzado-Alba, Sanz-Osorio & Laporta-Puyal, 2021, p. 7–17)

Some of the main characteristics of Si, SiC and GaN semiconductor materials are presented in Figure 6. Whereas the biggest differences between Si and WBG materials are the bandgap and critical field which allow WBG materials to have higher breakdown voltages, the main differences between SiC and GaN are with thermal conductivity and saturated electron drift velocity. These differences in WGB material characteristics determine that GaN devices are

more suitable for applications that require relatively low power and voltage but higher switching frequencies due to the high saturated electron velocity and electron mobility, whereas SiC devices on the other hand are better for applications that require higher power and voltage that produce more losses due to the highest critical field and thermal conductivity values of the three. Rough point to determine which technology should be used is 600 V and 1 kW (Millan, Godignon, Perpina, Perez-Tomas & Rebollo, 2014, p. 2155–2163)

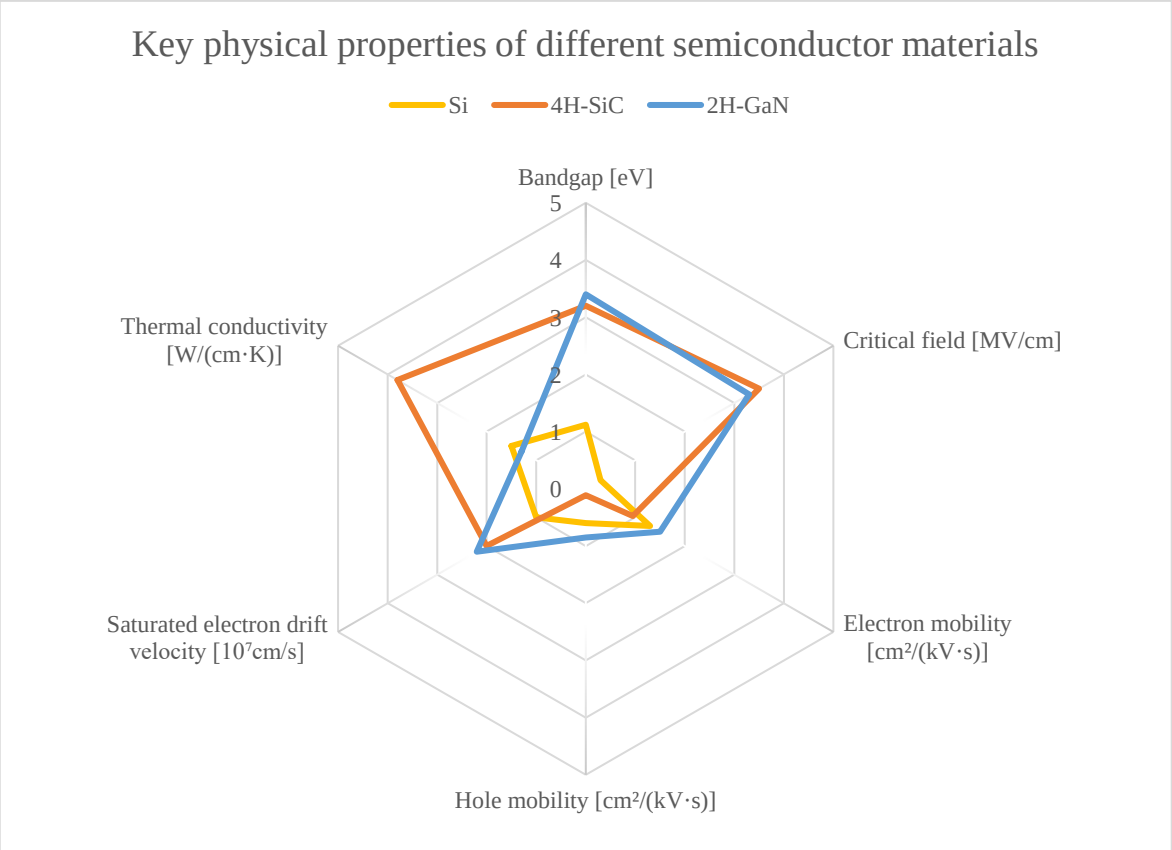

Figure 6. Key physical properties of Si, SiC and GaN semiconductor materials (Based on Lumbreras, Zaragoza, Mon, Galvez & Collado, 2019, p. 1)

According to the study conducted by Biela, Schweizer, Waffler & Kolar (2011) SiC devices offer significant benefits over the Si devices, especially, in high voltage converters. Wang et al. (2018, p. 1–12) conclude that as WBG semiconductors offer higher breakdown electric field, lower on-state resistance, faster switching speeds and can withstand higher junction temperatures than their Si counterparts, the power electronics converters can benefit from all these characteristics as they improve the efficiency, power density, specific power and

reliability of the end product. Dimitrijev (2012, p. 533–535) states that for example with SiC diodes it is possible to achieve on-state resistance that is only 1% of the on-state resistance of Si diodes while keeping the blocking voltage the same or reach even higher blocking voltages than possible with older technology while keeping the on-state resistance small.

Wang et al. (2018) conclude well why each of these characteristics are beneficial. Higher breakdown electric field of the WBG components allows them to be used in applications that require higher voltage. It also means that the component can be squeezed into a smaller package which can help decreasing the total volume of the system to some degree. However, the more important benefits of the WBG are their lower on-state resistance, faster switching speed and improved temperature capabilities which mean lower conducting losses, reduced size of the passive components and reduced cooling needs. These improvements can really affect the size of the total system and then improve the power density remarkably. (Wang et al, 2018, p. 1–12)

Road for the WBG technologies to overcome the Si technology however is not going to be easy. Since the WBG technologies are relatively new on the market and their market share is narrow, the price of these components is high when compared to well established Si-based components. Manufacturing processes need to be improved and optimized starting from the production of wafers to increase the yield and reduce the price, and like with all the new technology, the demand for these components must increase in order to get more manufacturers involved. On the other hand, the high price of the available components limits the interest and only niche sector can justify the higher price as it might be the only way to realize a certain design. Ballestín-Fuertes et al. (2021) conclude that EV sector might be one of the largest contributors to first adopt WGB and especially SiC technology during the coming years and decades thus increasing the development speed of it. (Ballestín-Fuertes et al., 2021, p. 7–17)

According to Wang et al. (2018) other challenges that WBG based design may face are the increased electromagnetic interference (EMI) emissions caused by higher voltage levels and switching frequency of WGB components which cause steeper du/dt and di/dt slew rates, high insulation requirements caused by the higher blocking voltage of WBG components and dozens of degrees higher junction temperatures than before. All these differences force the engineers applying WBG components to their design to consider the effect these changes

might have on how they are accustomed of designing things in order to use WBG components successfully. (Wang et al, 2018, p. 1–12)

2.1.5 Losses in a semiconductor switches

Mitigating losses as well as possible should be the goal while designing any device to improve its efficiency. In an ideal switch no current flows through the switch while it is open, its switching time is indefinitely short and there is no voltage drop across the switch while it is closed. In reality, any of these assumptions does not fully materialize and therefore there will always be losses. These losses caused by the semiconductor switches can be divided into switching P_{SW} and conducting losses P_{CON} determined whether the loss is introduced during the turn on or off of the switch or during its on-state where the switch is conducting.

Switching losses are caused by dynamic currents and voltages the switch must handle during its finite switching time.

$$P_{SW} = U_{DS} I_D f_{SW} \frac{(Q_{GD} + Q_{GS})}{I_G} \quad (1)$$

where P_{SW} is the switching loss (W), U_{DS} is the drain-to-source voltage (V), I_D is the drain current [A], f_{SW} is the switching frequency (Hz), Q_{GD} is the gate-to-drain charge (C), Q_{GS} is the gate-to-source charge (C), and I_G is the gate current (A).

Switching losses P_{SW} of a MOSFET can be defined by Equation (*1*). From Equation (*1*) it can be seen that the switching losses are a function of the voltage drop across the switch, drain current flowing through the switch, switching frequency and time it takes to charge the MOSFET defined by the total gate charges divided by the gate current. It can be concluded that the switching losses are defined both by the specs of the switch and the switching frequency. Even though Equation (*1*) suggests that a higher switching frequency always yields higher switching losses this is not completely true as the switching losses can be reduced or removed completely by utilizing soft switching methods which are presented later in this thesis.

Lakkas (2016) states that higher switching frequencies result in higher gate-drive losses which is one of the reasons why efficiency of the switch is reduced when switching frequency in increased. He also points out that the characteristics of a switch are always a trade-off between multiple parameters of it. When the size of the MOSFET is increased to provide smaller on-state resistance $R_{DS(on)}$ and conducting losses P_{CON}, the gate capacitances are increased resulting in higher switching losses P_{SW}. (Lakkas, 2016, p. 22–26)

$$P_{\mathrm{CON}} = R_{\mathrm{DS(on)}} I_{\mathrm{D}}^2 \tag{2}$$

where P_{CON} is the conducting loss of the semiconductor switch (W), $R_{DS(on)}$ is the on-state resistance of the semiconductor switch (Ω) and the I_D is the drain current which is flowing through the switch (A).

The conducting loss P_{CON} can be defined with Equation (*2*). Conducting losses in the semiconductor switch are caused by the voltage drop U_{DS} across the switch while it is conducting. This voltage drop is caused by the on-state resistance $R_{DS(on)}$ which is a defined parameter for the selected semiconductor switch.

Lumbreras et al. (2019) have conducted simulations of two- and three-level power converters using both Si and WBG based semiconductors at different modulation methods and switching frequencies ranging between 50 – 500 kHz. Their results can be summarized so that with Si based two-level converters using sinusoidal PWM and simulated at switching frequencies of 50 and 100 kHz, the switching losses are approximately 35 and 100 times as high as the conducting losses depending on the switching frequency respectively, showing that the higher the switching frequency is increased the more dominant the switching losses naturally become. With WBG based converters the situation is a bit different as with lower switching frequencies of 50 kHz the conduction losses and switching losses are of the same magnitude. However, when the switching frequency is increased the switching losses also increase linearly. The results of their study however show that the losses of a WBG based converter at high switching frequency of 500 kHz are still less than half of the same of a Si based converter at 50 kHz. (Lumbreras et al. 2019, p. 1–7)

2.1.6 Switching methods

As stated in the earlier chapter the semiconductor switch losses can be divided into switching and conducting losses. Whereas conducting losses are dependent on the characteristics of the semiconductor component parameters which cannot be modified by the end user, there are ways to mitigate the switching losses. Switching losses could be reduced by decreasing the switching frequency as described in the earlier chapter but generally most applications benefit from having a higher switching frequency, which allows smaller passive components to be used and, as a result, a smaller volume of the total system can therefore be achieved. Therefore, a better way to mitigate switching losses is to alter how the switching is made. Switching methods can be divided into hard switching and soft switching where hard switching may in most cases be the easiest to implement but causes the highest losses since no actions are taken to reduce switching losses.

Figure 7 presents the losses of a hard-switched single switch part of full-bridge converter's leg. In Figure 7 it can be seen that once the switch is set to conduct by sending a control signal to turn it on, there is a time delay $t_{d(on)}$ before the drain current I_D starts rising. The current I_D reaches it maximum value in t_{ri} after which the voltage across the switch starts decreasing. It takes t_{fu} for the voltage to reach its on-state value U_{on} which is defined by the on-state resistance R_{on} of the switch and the drain current I_D. Switching on losses are caused because the voltage U_D starts to decrease only after the current I_D has reached its maximum value and the energy lost in switching on can be calculated by calculating the area of the triangle $E_{c(on)}$.

Conducting losses can also be seen from the Figure 7. After the switch has been turned on and voltage U_D has reached its on-state value U_{on}, it will have the same value given that the on-state resistance R_{on} and drain current I_D are kept the constant for the whole period during which the switch is conducting, here defined as t_c. On-state losses can now be calculated from the area of the E_{on}.

Switching losses when the switch is opened are formed in the similar way as when it is closed. As seen in the Figure 7. after receiving the control signal to turn off there is a time delay $t_{d(off)}$ after which the voltage U_D start rising during t_{ru}. As the voltage U_D reaches its

maximum value the drain current I_D starts decreasing during t_{fi}. Again, the switching loss during the switch is being turned off can be calculated from the area of $E_{c(off)}$.

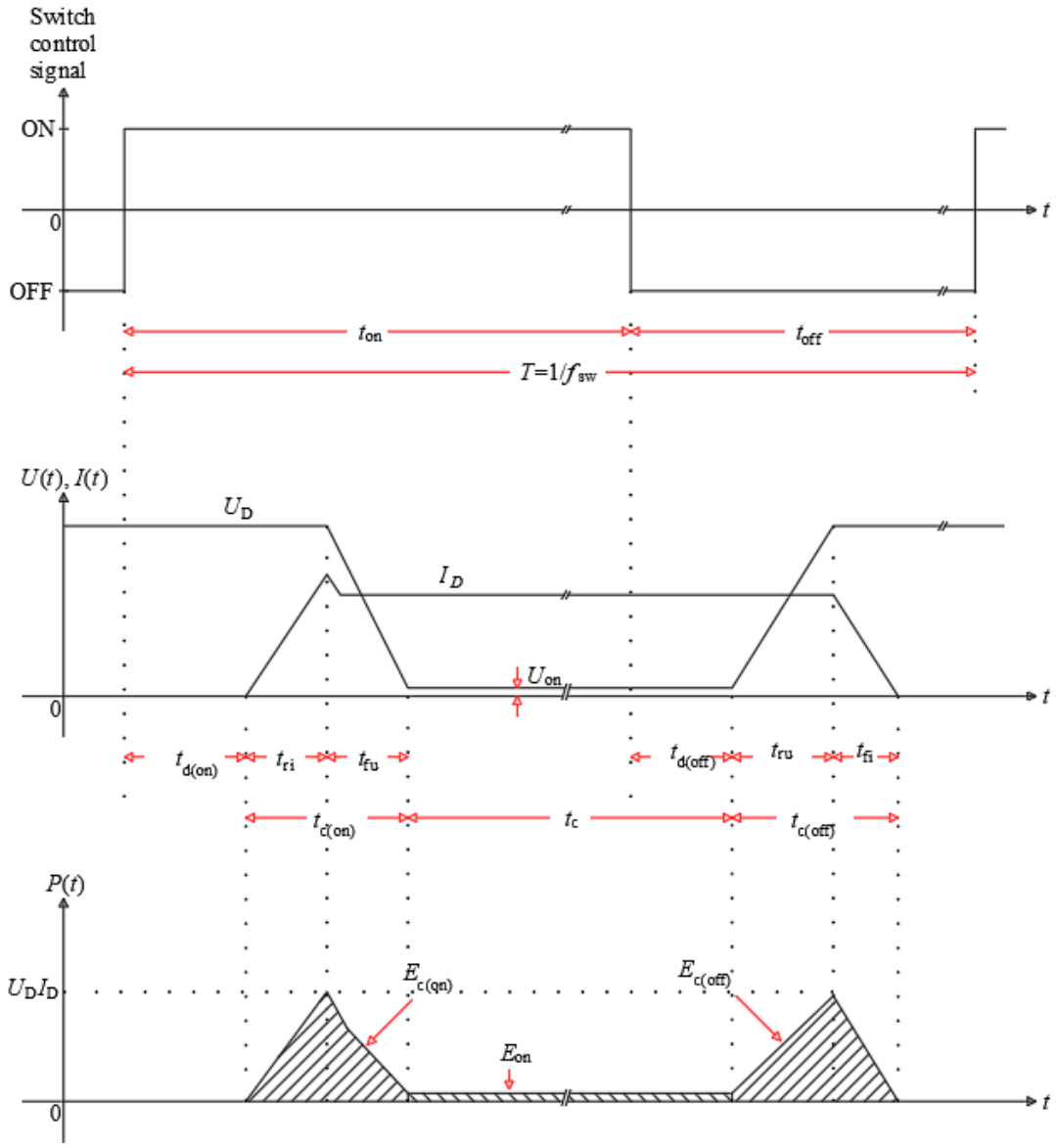

Figure 7. Losses of a hard-switched switch.

Switch stresses can be reduced by utilizing so called dissipative snubber circuits built out of diodes and passive components which are connected in series and parallel to the switches. The use of these snubber circuits does not however improve the efficiency of the total converter, but the switching losses are transferred from the switch to the snubber circuit. (Mohan, Undeland & Robbins, 1995, p. 251)

In order to decrease the switching losses soft switching techniques such as Zero Current Switching (ZCS) and Zero Voltage Switching (ZVS) can be utilized. In ZCS and ZVS the semiconductor switch is turned on or off so that either the switch is not conducting current at the same time as the voltage across it is decreasing or increasing or the voltage across the switch is ideally zero while the current flowing through it is decreasing or increasing thus reducing switching losses, switch stresses and EMI. Figure 8 gives yet another overview of the turn-on and turn-off loci of a switch that utilizes either hard switching, soft switching or snubber circuits. As will be seen later on when presenting different converter topologies, soft switching can be achieved either with suitable topology, control method, additional resonant circuits, or different combinations of these. (Wintrich, Nicolai, Tursky & Reimann 2015, p. 3–4; Mohan et al., 1995, p. 249–294)

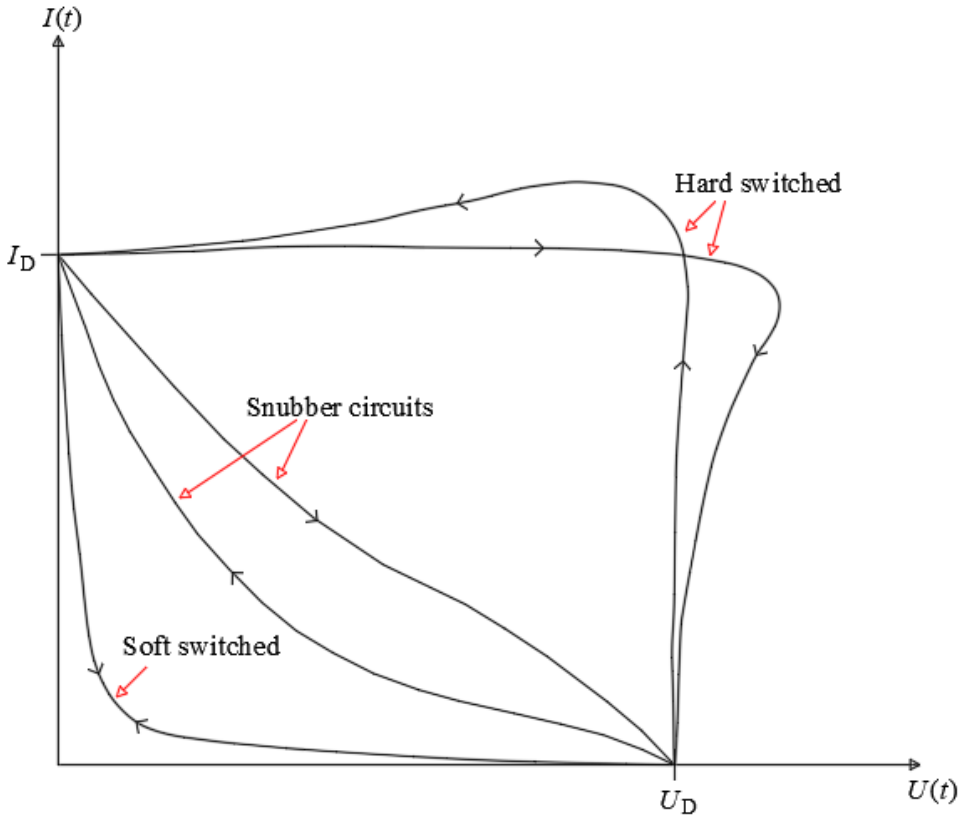

Figure 8. Switching loci of a hard switched switch, soft switched switch, and a switch with snubber circuit. Adapted from Mohan et al., 1995)

2.2 Discrete passive components

All converter topologies require discrete passive components in addition to semiconductor switches to operate. These passive components can be divided further into magnetic and capacitive components, which are covered in this chapter. The focus is on what kind of properties of these components are essential in a high-power DC-DC converter application.

2.2.1 Magnetic components

Different kinds of magnetic components, including inductors and transformers, are utilized in converters. Inductors are used for momentary storing of energy, and they can be utilized as chokes that stabilize the current. Inductors may also be part of filter circuits or in some topologies they are used as part of resonant circuits which are utilized to achieve soft switching. Transformers are utilized mainly to provide galvanic isolation and to provide voltage or current transform ratio suitable for the application. Ideal transformer does not store any energy in its windings but passes it through from the primary winding to its secondary winding immediately. In practice, some energy is always stored in the stray and magnetising inductances of the transformer. Some topologies such as flyback converter utilise transformer like coupled inductors which are used to store energy momentarily and provide galvanic isolation.

Erickson et al. (2020, p.444–451) describe some of the challenges and constraining factors that one must think of while designing a magnetic component for a converter. Choosing a suitable component is not just a matter of selecting an inductor with a suitable inductance or a transformer with a suitable turns ratio, but one must also consider saturation of the core material, core and copper losses, whether or not an air gap is required in the core, the size and shape of the core and its window and so on. Given this, one could understand that the design of the magnetic components for a converter is a challenging and important part of the converter design as in most cases suitable components cannot be found of the shelf, but they need to be tailored to match the application.

The design of the magnetic components plays a significant role in determining the power density and specific power of the converter. Since copper is typically used in windings and magnetic steel or different other ferromagnetic alloys as the core material, the effect the size

of the magnetic components have on the mass of the converter is obvious. By increasing the switching frequency, the amount of energy required to be stored in the inductor is decreased thus decreasing the required inductance. High frequency transformers allow smaller volume, lighter weight, and lower cost when compared to low frequency transformers. Additional benefits such as avoiding distorted voltage and current waveforms due to core saturation and lack of audible switching noise when the switching frequency is over 20 kHz are also worth mentioning. (Zhao, Song, Liu & Sun, 2014).

According to Erickson et al. (2020) inductor's losses can be divided into copper losses and core losses. Copper losses are caused by the AC resistance in the inductor winding and therefore they can be described as a resistor which is connected in series with an ideal inductor. Copper losses could be reduced by increasing the cross-section of the wire used in the winding, i.e. by adding more copper. This, however, increases the mass, size and the cost of the inductor or transformer.

Copper losses can be increased also because of skin and proximity effects, both of which are caused by eddy currents and become more and more dominant as the cross section of the conductor increases. Skin effect causes the current flowing in the conductor to pack to its surface if the frequency of the current is increased high enough, i.e. the current density in the conductor is not distributed evenly but it is higher at the surface, and especially in possible corners, thus decreasing the effective cross section of the conductor. Suspended in free air a metal has a skin depth

$$\delta = \sqrt{\frac{\rho}{2\pi\mu f}} \tag{3}$$

where δ is the penetration depth (m), ρ is resistivity (Ωm), μ is permeability (H/m), and f is frequency (Hz).

Penetration depth calculated with Equation (3) for certain conductor material operated at certain frequency f describes at which depth the current is decreased to $1/e$ when compared to current at the surface of the conductor. By comparing the penetration depth to the thickness of the conductor it can be judged if the skin effect causes noticeable increase in the resistance of the conductor thus increasing the losses. According to Nan & Sullivan (2009) the increased losses caused because of the skin effect can be mitigated by using litz-

wire windings which are formed out of many thin transposed strands that have smaller diameter than the penetration depth.

Proximity effect is a phenomenon which causes additional current to be induced from one conductor to another at its close proximity thus increasing the current flowing in the conductor and the losses in it. According to Erickson et al. (2020, p.426–430) the proximity effect causes additional losses in multilayer windings of the transformers and inductors operated at high frequencies when the thickness of the conductor $h >> \delta$.

$$P = I^2 \left(\frac{h}{\delta} R_{\mathrm{DC}}\right) \sum_{m=1}^{M} [(m-1)^2 + m^2] \quad (4)$$

where P is the total copper loss (W) in an M layer winding, I is the RMS current flowing in the first layer winding (A), h is the thickness of the conductor (m), δ is the penetration depth (m), R_{dc} is the DC or low frequency resistance of the conductor (Ω), and M is the total number of layers.

By substituting the number of winding layers into Equation (4) derived by Erickson et al. (2020, p.430) it can be seen that for example for a two layer winding the copper losses caused by the proximity effect increases the losses to be six times as high as with a single layer windings. According to Erickson et al. (2020, p.438–441) the losses caused by the proximity effect can be mitigated by utilizing interleaved windings in which the primary and secondary windings are wound so that they are altered on the core.

Core losses then again are caused by the eddy currents in the core of the inductor. Changing the magnetization of the core requires energy of which part is recovered but another part lost as a heat. This power loss is shown as a hysteresis of the flux density (B) - magnetic field (H) loop, which describes the unideal dependency between the magnetic field strength and flux density of a magnetic core material. Erickson et al. (2020) state that while designing an inductor, a trade-off must be made between the core losses and high saturation flux density. The size, weight and cost of the inductor can be reduced when inductor is designed to have a high operating flux density. According to Erickson et al. (2020) high flux densities can be achieved with core material such as silicon steel, but these materials also cause high losses due to their low resistivity, which causes high eddy currents thus making it suitable for low frequency applications in which the eddy current losses are not that significant. Cores can be built out of laminates which help to reduce the eddy currents as the increased resistance

between the laminates decreases the eddy currents. Other core materials and types such as powdered cores, amorphous alloy cores and ferrite cores offer lower saturation flux densities and higher resistivity, and therefore the core losses can be smaller. Each of these materials have their own advantages and disadvantages which make them suitable for a certain application with a certain switching frequency. For example, Ericson et al. (2020) state that manganese-zinc ferrite cores are commonly used in transformer and inductor cores of converters operated at 10 kHz to 1 MHz switching frequencies. (Erickson et al., 2020, p.423–425)

2.2.2 Capacitors

Capacitors serve many purposes in DC-DC converters. They can be used for example to filter the input and output voltages of converter, as part of resonant converters' resonance circuits or as part of snubber circuits.

According to Kazimierczuk (2016), the important factors for capacitors used in converters and power electronics in general in addition to its capacitance *C*, are its equivalent series resistance (ESR), equivalent series inductance (ESL), self-resonant frequency, and breakdown voltage. ESL is formed from the stray inductances in the structure of a capacitor such as its conductors. This additional inductance will be connected in series with the capacitor as the name implies and it must be taken into consideration when dimensioning a converter. Kazimierczuk (2016) states that depending on the topology this may or may not have a negative effect on the operation of the converter. (Kazimierczuk, 2016, p. 115–116)

ESR is as well caused by stray resistances in the structure of a capacitor such as the resistance of the contacts, leads and plate conductors and these resistances are also connected in series to its capacitance and ESL. Mack (2005) states that ESR is important parameter because it affects the ripple current capability of the capacitor. The AC current flowing through ESR causes losses in the capacitor and therefore low ESR values are to be pursued. ESR value of a capacitor depends highly on the type of the capacitor and the operating conditions.

Breakdown voltage determines how high voltage can be applied across the capacitor before a breakdown occurs in its dielectric material. Dielectric material and its thickness determine

capacitor’s breakdown voltage. In addition to parameters mentioned Kazimierczuk (2016) the volume of the capacitor and its price are factors to consider when selecting a capacitor.

Electrolytic capacitors are commonly used also in power electronic applications because they are inexpensive and offer a high capacitance packed in low volume. Mack (2005) states that the advantages of electrolytic capacitors are that those can be manufactured for large capacitance and high voltage rating and their size is small. According to Mack (2005) the lifetime of electrolytic capacitors may be one of its weakest properties and therefore sufficient cooling is required to achieve tolerable lifetime in applications which require continuous operation.

Katzimierczuk (2016) mentions thin film capacitor as another capacitor type that offers high breakdown voltage and suitable capacitance required for such a high-power high-voltage converter. It has more stable capacitance over different operating condition, increased lifetime and reduced ESR when compared to electrolytic capacitors, but on the other hand film capacitors are more expensive and have larger volume when compared to electrolytic capacitors of similar capacitance.

2.3 Parallel and series connection

Parallel connection can be used to increase converter’s current rating and hence the power it can output. This can be done on many levels starting from connecting multiple chips, modules or converters in parallel. Parallel connection enables also interleaving which means distribution of duty cycles by phase shifting. This increases the apparent switching frequency of the total system, which is beneficial for the quality of output voltage and current waveforms and hence can be used reduce the need for output filtering. For some high-power applications parallel connection is the only possibility to reach the required power level as components rated for high enough current may not be available. However, regardless of the benefits the parallel connection offers its feasibility for lower power applications just to improve the output voltage quality is limited because of the additional costs it adds when compared to just using simply larger passive components.

In order to reduce the voltage stress individual switches need to withstand, series connection can be utilized. For series connected switches the voltage across each switch is inversely

proportional to number of series connected switches. Series connection enables the use of lower voltage rated components to reach required voltage level which is beneficial for applications where components with high enough voltage rating are not available. Use of lower voltage rated components such as multiple series connected MOSFETs instead of a single IGBT with higher voltage rating could be also beneficial in some applications to reach higher switching frequencies or lower on-state resistance while keeping the voltage rating high. On system level multiple converters can be connected in series either to achieve features that are not possible or practical to achieve with a single converter. For example, in applications in which extreme conversion ratio, high input voltage, galvanic isolation or different combination of these is required it could be feasible to use two DC-DC converters with different topologies connected in series to optimize the design.

2.4 Converter topologies

There are many different types of converter topologies which all have a different characteristic over another and are hence suitable for different types of applications. Some might be used bi-directionally to provide power flow from primary stage to secondary stage and vice versa while others work only unidirectionally, some provide galvanic isolation between the primary and secondary stages and some converter topologies allow step-down, step-up or even both conversion modes. Others have single input and single output, while other may provide multiple outputs for different voltage levels. Nayanasiri & Yunwei (2022) for example have written a good overview of different DC-DC step-down converter topologies which presents the key features of many different type topologies.

A few of the most common step-down converter topologies are Buck converter, Flyback converter and different types of Half-Bridge and Full-Bridge converters that come in a number of different variations. The simplest form of converters can be built using very few basic components such as capacitor, inductor, diode, and a single semiconductor switch. By increasing the number of components additional features such as isolation, bidirectionality or higher voltage and power rating can be achieved but simultaneously the complexity of the hardware and especially its control system is increased.

In this thesis the basic structure and control concept of a few common DC-DC step-down topologies is presented. More detailed presentation of different topologies in which for

example voltage transfer functions of different converter topologies are derived, different operating principles are described and design methods are presented is left for the referred literature such as Kazimierczuk (2016), Erickson et al. (2020), Ang & Oliva (2010) or Brown, Kularatna, Mack & Maniktala (2008).

2.4.1 Buck converter

Buck converter which is also called as step-down converter is one of the most commonly used converter topologies in the world and one of the reasons for it is its versatility. Buck converter has a very simple construction, and it can be used in multiple different applications ranging from few watts electronic circuit converters to tens of kilowatt high power converters. Being a step-down converter, its average output voltage is always lower than its input voltage. Buck converter in its basic form provides only unidirectional power flow with no isolation.

The structure of buck converter is shown in Figure 9. According to Kazimierczuk (2016), a buck converter consists of a switch S_1 and a freewheeling diode (FWD) D_1, which are used to control the energy flow from the source to the load and an inductor L_1 and an output capacitor C_{OUT} which are used to store and transfer energy.

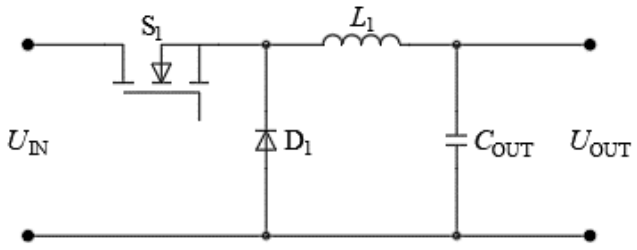

Figure 9. Buck converter topology.

Buck converters can be switched using either hard or soft switching. In the study conducted by Alavi et al. (2020), multiple methods including their own proposal for soft switching of buck converter are presented. According to their conclusion soft switching can be implemented either with sophisticated control methods or by adding different types of resonant circuits to the converter. Some of the presented methods, however, provide only

partial soft switching, introduce high stresses on the switch components or are complex to control. (Alavi, P., Babaei, E., Mohseni, P. & Marzang, V., 2020, p. 1456–1465)

A hard switched buck converter can be controlled by controlling S_1 with a pulse width modulated (PWM) control signal which has a duty cycle *D*. Duty cycle is a ratio of switch conducting time t_{on} and period *T*, which is an inverse value of the switching frequency f_{sw}. Duty cycle is defined by

$$D = \frac{t_{\mathrm{on}}}{\mathrm{T}} = \frac{t_{\mathrm{on}}}{t_{\mathrm{on}}+t_{\mathrm{off}}} = t_{\mathrm{on}} f_{\mathrm{sw}} \tag{5}$$

In hard-switched buck converter the output voltage is directly proportional to the product of duty cycle and input voltage

$$U_{\mathrm{OUT}} = D U_{\mathrm{IN}} \tag{6}$$

where U_{OUT} is the output voltage (V), *D* is the duty cycle and U_{IN} is input voltage (V).

Equation (6) presents the voltage transfer function of a lossless buck converter in continuous conduction mode (CCM) where current is flowing continuously through inductor L_1. The output voltage U_{OUT} of a buck converter can theoretically vary between 0 – U_{IN} by altering *D* from 0 to 1 when operating in CCM but according to Kazimierczuk (2016) it practically can vary between 5 – 95% of U_{IN}. Discontinuous conduction mode (DCM) in which current does not constantly flow through L_1 is not discussed in this thesis as it is generally possible only with light loads and has been described by Kazimierczuk (2016, p. 108–110).

2.4.2 Buck-boost converter

Similarly to buck converter, a buck-boost converter is an unidirectional and un-isolated topology which is widely in use in different applications due to its simple design. Buck-boost converter is a cascade connection of buck and boost converters, so its structure and the components utilized are very similar to ones of a buck converter. Similar components are used but the places of FWD D_1 and inductor L_1 are switched. This change allows the buck-boost converter to be used either to step down or to step up the input voltage. Another difference to buck converter is that the polarity of the buck-boost converter's output is

reversed in relation to polarity of the input. The structure of a buck-boost converter is presented in Figure 10.

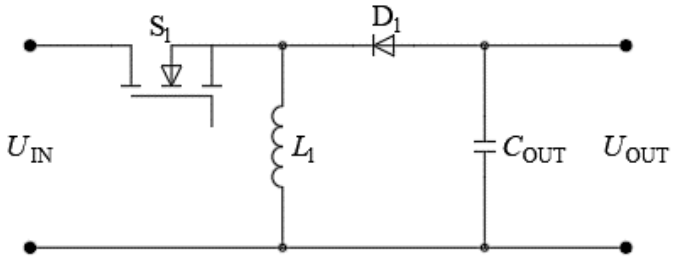

Figure 10. Buck-Boost converter topology.

Hard-switched buck-boost converter can also be controlled by altering its duty cycle, but its voltage transfer function differs from Equation (6) and is define by

$$U_{\mathrm{OUT}} = \frac{D}{1-D} U_{\mathrm{IN}} \tag{7}$$

where U_{OUT} is the output voltage, D is the duty cycle and U_{IN} is the input voltage.

Equation (7) presents the voltage transfer function of a lossless buck-boost converter operated in CCM. From Equation (7) it can be seen that when $D < 0.5$ the converter is operated in buck mode, when $D > 0.5$ the converter is operated in boost mode.

2.4.3 Flyback converters

Flyback converter is a simple converter topology which is very similar to buck-boost converter. It shares mostly same components, but the inductor has been replaced with a coupled inductor to provide galvanic isolation. Due to similarity with the buck-boost converter, Kazimierczuk (2016) actually describes the flyback converter as an isolated version of a buck-boost converter. The coupled inductor used in a flyback converter can be referred to also as flyback transformer and it is inversely wound so the polarity of the output voltage is not reversed like in buck-boost converter.

The advantage of the flyback topology is that the count of its components is low when compared to other isolated converters. Only one switch is used, and no inductor is needed in addition to the coupled inductor. Partly therefore also the size of the converter is small, and its price is low. Having multiple different outputs with different output voltages is also simple and requires only additional secondary stages to be added to the common core. However, according to Erickson et al. (2020) and Tamyurek & Kirimer (2015) the high voltage stress on the switch and challenging design of the flyback transformer causes the flyback converters typically to be used only in low power applications.

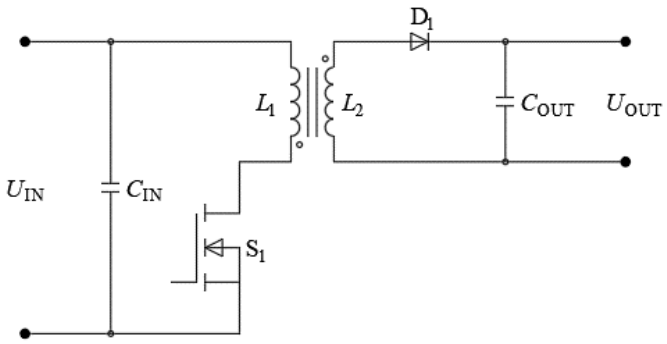

Figure 11. Flyback converter topology.

The voltage transfer function of a hard switched flyback converter can be defined by

$$U_{\mathrm{OUT}} = n\frac{D}{1-D}U_{\mathrm{IN}} \tag{8}$$

where U_{OUT} is the output voltage (V), n is the turns ratio of the coupled inductor, D is the duty cycle of the switch, and U_{out} is the output voltage (U).

The voltage transform function for flyback converter shown in equation (8) is the same as the equation (7) for buck-boost converter, but with additional turns ratio n.

2.4.4 Hard switched full-bridge converters

A full-bridge converters come in variety of different forms. Hard-switched full-bridge converter topology is presented in Figure 12 in which the primary stage has an active H-

bridge inverter, secondary stage has a passive rectifying diode bridge, and the switching stages are separated by a high frequency transformer. The primary stage is a single-phase inverter consisting of four switches S_1-S_4 with free-wheeling diodes (FWD) D_1-D_4 and an input capacitor C_{IN}. The secondary stage is a passive single-phase rectifier consisting of four diodes D_5-D_8 and a low-pass filter (LPF) formed out of L_1 and C_{OUT}. Because the secondary stage is built using diodes instead of active switches, the full-bridge converter provides only unidirectional conversion. The high frequency transformer T_1 between the primary and secondary stages transfers energy between the stages and provides isolation and required turns ratio.

Fan, Pu, Liu, Ma, Li & Williams (2014) studied the suitability of hard switched full bridge converter in high-power and high-voltage wind-energy application. They came to conclusion that even though topologies such as simple single-switch boost converter may provide better efficiency or more complex full-bridge topologies would enable soft switching, the hard-switched full-bridge topology offers good functionality for reasonable cost, especially, for lower switching frequencies.

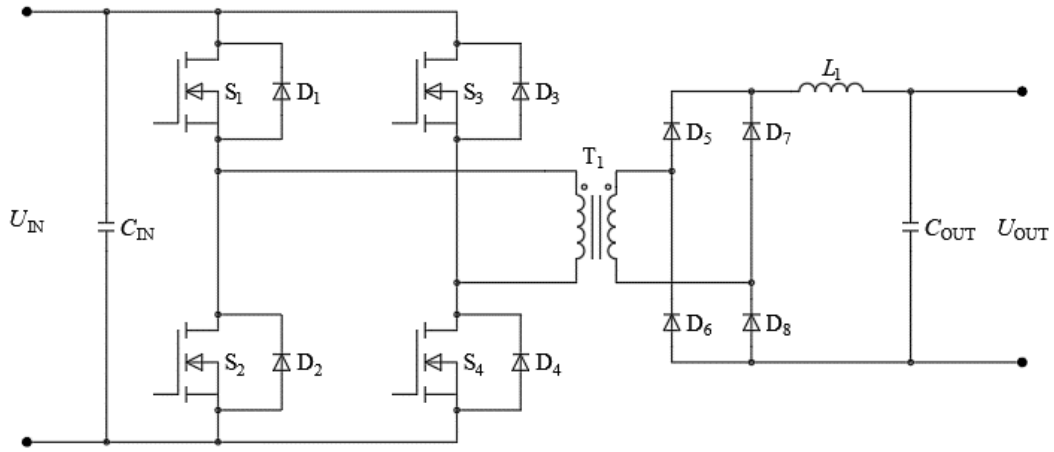

Figure 12. Full-bridge converter topology.

Full-bridge converter can be operated by hard switched PWM method or more sophisticated methods such as phase shifting method which allows soft switching. In both methods the switches are operated in pairs so that switches S_1 and S_4 form one pair and switches S_2 and S_3 the another. Switches are operated so that series connected switches of the same leg are never conducting at the same time. This dead-time, during which neither of the switches of

the same leg are conducting, prevents short circuiting the leg and thus the input of the converter by allowing the switch component to be fully turned off before next switching action is made. The output voltage of a hard switched full-bridge converter is determined by it input voltage, the duty cycle of the switches and the turns ratio of the converter, and it is defined as

$$U_{\mathrm{OUT}} = U_{\mathrm{IN}} D n \tag{9}$$

where U_{OUT} is the output voltage (V), U_{IN} is the input voltage (V), D is the duty cycle, and n is the turns ratio of the transformer.

2.4.5 Full-bridge resonant converters

Resonant converters come in variety of different configurations and on the first glance they seem very similar to hard-switched full-bridge converter. However, resonant converters have a resonant tank connected in series with the windings of the high frequency transformer and they lack the inductor at the output. Resonant converters can be classified according to their resonant tanks and hence they are named as series resonant converter, parallel resonant converter, LLC resonant converter, CLLC resonant converter and so on. On most variations the resonant tank is only on the primary side of the transformer but there are exceptions such as CLLC converter which has resonant circuits connected in series to both sides of the transformer. LLC resonant converter is used as an example of resonant converters in this thesis and it is presented in Figure 13.

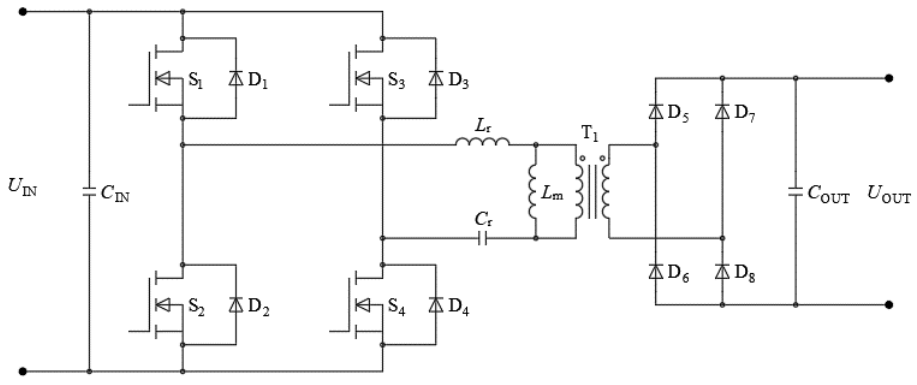

Figure 13. LLC resonant converter topology.

Guo & Sha (2020) and Barbi & Pöttker (2018) have written books about soft switched isolated DC-DC converters in which they describe different topologies and control methods for these. Different variations of resonant converters are also included. Mohan et al. (1995) state that resonant converters in general combine resonant circuits and switching strategies to achieve ZVS, ZCS or both of these. Guo et al. (2020) continue that LLC resonant converters for example can achieve ZVS for inverter side MOSFETS and ZCS for rectifying diodes.

Barbi et al. (2018) state that LLC resonant converters can be controlled either with PWM or with frequency modulation (FM). In FM control the output voltage of the converter is controlled by adjusting the switching frequency f_{SW} in relation to the converter resonant tank's resonance frequency f_r. According to Barbi et al. (2018) the output voltage of the LLC resonant converter can be defined as

$$U_{OUT} = \frac{\sqrt{\left(\frac{f_{SW}}{f_r}\right)^4 - \frac{\pi^4}{64}\left[\left(\left(\frac{f_{SW}}{f_r}\right)^4 - 1\right) I'_{OUT}\right]^2}}{\left(\frac{f_{SW}}{f_r}\right)^2 (\lambda + 1) - \lambda} U_{IN} \quad (10)$$

where U_{OUT} is the output voltage (V), f_{SW} is the switching frequency (Hz), f_r is the resonance frequency (Hz), I'_{OUT} is the normalized average value of output current referred to transformer's primary side (A), and λ is the ratio of resonance inductance L_r and magnetizing inductance L_m.

Equation (10) shows that the voltage gain of LLC resonant converter depends on dimensions of the resonant tank components that affect the f_r and λ, transformer's turns ratio, and the operation conditions that affect the U_{IN} and I'_{OUT}.

Guo et al. (2020) state that LLC resonant converters are great for applications in which fixed, or relatively narrow conversion ratio is required as then the frequency tank can be dimensioned for that specific ratio and optimal performance can be achieved. If wider voltage range is required, the converter needs to operate at wider switching frequency range which reduces its efficiency. Therefore, LLC resonant converter is at its best when it is operated at fixed conversion ratio so that it provides isolation and cascaded non-isolated converter handles the output voltage regulation. (Guo et al., 2020, p. 8 – 9)

2.4.6 Dual Active Bridge converter

Dual active bridge (DAB) converter is a symmetric topology that consist of two actively switched converter stages separated by a high frequency transformer as shown in Figure 14. The primary stage has the same H-bridge as in full-bridge converter and it consists of four switches S_1-S_4, their FWDs D_1-D_4 and an input capacitor C_{IN}. The intermediate stage has a high frequency transformer T_1 which transfers energy between the switching stages and provides isolation as in full-bridge converter, but in addition a magnetising inductor L_1. The secondary stage differs also from the full-bridge converter as instead of passive rectifier circuit it is has an active switching circuit consisting of switches S_5-S_8 and FWDs D_5-D_8. Secondary stage also has only output capacitor C_{OUT} instead of LPF. Since both stages are actively switched the converter can be used bidirectionally.

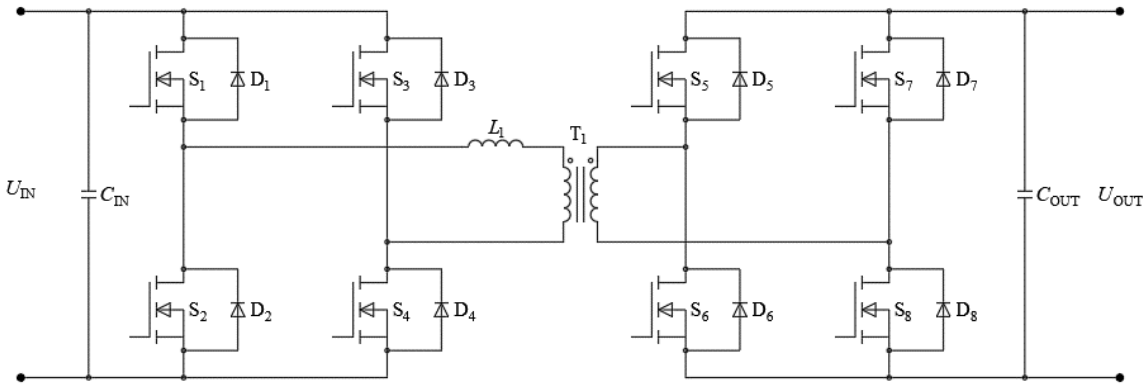

Figure 14. Dual active bridge (DAB) converter topology.

According to Zhao et al. (2014) DAB converter was introduced in early 1990's but only the recent advances in wide bandgap semiconductor and magnetic materials enabling it to become more efficient have made it gain more attraction.

DAB converters are typically controlled with different types of phase shift modulation methods. Zhao et al. (2014) describe the single-phase-shift (SPS), dual-phase-shift (DPS), extended-phase-shift (EPS) and triple-phase-shift (TPS) control methods as the most studied methods at the time of writing their article. In SPS which is the simplest methods of these four, the duty cycle of the switches is kept constant 0.5 and by adjusting just the phase shift

between different conducting switch pairs the power flow and its magnitude can be altered. According to Zhao et al. (2014) even the SPS control allows soft switching for limited power range but in order to gain soft switching for wider power range, reduce component stresses, reach better efficiency, and reduce the size magnetic and capacitive components other, more complex, control methods need to be used. (Zhao et al., 2014, p. 4095–4096)

DAB converter can be used a base for different variations of resonant converters which include resonant tanks such as LC and CLLC. With the aid of these resonant tanks for example the efficiency of the converter can be improved by extending the soft switching range and reducing the circulating currents. Zhao et al. (2014) present the said variations and their key benefits. For example, with LC resonant topology, which resembles unidirectional series resonant converter, ZVS for primary side switches and ZCS for secondary side switches can be achieved. This converter can be operated with a phase-shift control in which the switching frequency is kept fixed. Different CLLC variations then again can achieve soft switching for even wider power range which is beneficial for high power applications which require wide voltage and power range. According to Zhao et al. (2014) CLLC converters are operated with frequency modulation control which increases the complexity of the control even more. The additional parts required for the resonant tanks increase both the price and required volume for these resonant converters when compared to basic DAB converter. (Zhao et al., 2014, p. 4096-4097)

3 DC-DC converter comparison

In this chapter the requirements of the DC-DC converter for Epiroc's trolley use case are discussed and defined after which a market study is conducted to understand the availability of these kinds of converters on the market. Finally, some of the most promising findings are presented and compared against the requirements and against one another.

3.1 Special requirements of the Epiroc's NRMM application

The requirements set for the DC-DC converter of a mining truck are presented in this chapter. Both the mechanical and electrical requirements for the converter originate from the challenging operating environment, existing design of the base truck to which the converter must adapt to, electrical interface of the OCS and standardization which must be followed.

3.1.1 Mechanical requirements

One of the most important characteristics for a converter designed for NRMM application is its ability to withstand the harsh environment it is meant to be operated in. In mining environment, the most decisive parameters are the ambient temperature, shocks and vibrations, humidity and condensation, corrosive liquids and gasses and possibly high altitude.

Since the truck is operated outdoors both underground and on the surface around the year it must be able to handle wide range of ambient temperatures ranging from northern hemisphere's winter temperatures to the temperatures of deep underground mines. In practice this could mean ambient temperature range of at least -20…+50 °C but even higher or lower temperatures are possible in extreme cases. The ambient temperature must be taken into consideration when designing the cooling system of the converter as it is one of the environmental parameters that has the most effect on the cooling system's dimensioning. The effectivity of the cooling system after all determines the lifetime of the converter, since as a rule of thumb, every 10 °C increase in the component's temperature reduces its lifetime in half.

The ambient temperature can also change quite rapidly from another end of the scale to the other meaning that it is possible that during a half an hour drive from underground to the surface the ambient temperature can change well over 60 °C and then heat up the same amount when driving back during the next half an hour. This affects how humidity is condensing inside the converter, how different materials age and so on. Changing temperatures especially when decreasing past dew point lay the converter open to condensation which affects pollution degree and must be accounted when clearance and creepage distances are defined so that risk of short circuits is mitigated. There must also be a way to lead this condensed humidity out of the converter.

As a rule of thumb, the deeper the mine is, the higher its ambient temperature gets. The temperature inside a mine rises by 1 °C every 100 m the mine extends deeper underground. Mines also are excavated deeper as they deplete so on average the depth of the mine increases 30 m every year which translates to 0.3 °C increase in the maximum ambient temperature every year. This must be accounted so that the cooling system is not under dimensioned for the future needs.

Another parameter that affects the machine's cooling system dimensioning is the maximum altitude at which the machine is operated at. As the altitude increases the air gets thinner which directly affects how large air mass can be moved with cooling fans. In certain mines altitudes of 4 km above mean sea level (AMSL) or even higher are possible which would set tough requirements for the system but for the mine where the first trolley truck is intended to be used at first the maximum altitude of 1000 m is sufficient. However, for futureproofing the system, it should be designed using the maximum altitude at which the machine is to be operated as a base value for the calculation. The effect the altitude has on the isolation strength will be considered in the following chapter where electrical requirements are considered.

As one can understand when considering the mining industry and earth-moving applications mud and dust are present at all times. Both wet mud and possibly conductive dust must be kept out of the converter, so a dust proof enclosure is needed. Therefore, an IP6X rated protection is required which according to Table 1 means that the cabinet is dust-tight.

Table 1. Elements of the IP code according to EN 60529.

Numeral	First number (IP#X) Protection against ingress of solid foreign objects	Second number (IPX#) Protection against ingress of water
0	non-protected	non-protected
1	≥ 50 mm diameter	vertically dripping
2	≥ 12.5 mm diameter	dripping (15° tilted)
3	≥ 2.5 mm diameter	spraying
4	≥ 1.0 mm diameter	splashing
5	dust-protected	jetting
6	dust-tight	powerful jetting
7	-	temporary immersion
8	-	continuous immersion

As the truck is used outdoors and underground all around the year the converter must be able to handle humidity and moisture caused by rain and water table dripping inside the mine well. Practically this means that the converter must be cased inside a waterproof enclosure. Converter should be able to be washed with a pressure washer during regular cleaning of the truck so IPX5 rating should be met at minimum which according to Table 1 means that the cabinet is protected against jetting.

Converter requires active cooling due to high power loss of dozens of kW. Liquid cooling is required due to its higher effectivity when compared to forced air cooling, which is caused by the higher thermal conductivity of liquids when compared to gases. Also, the dust and waterproofed cabinet makes the forced air cooling of the converter in such dirty environment hard and impractical. It is suggested that the converter should be connected to an existing cooling circulation of the machine for easy implementation. However, if the losses of the converter are so high that the existing cooling system is not sufficient to cool it, the converter needs to have its own closed loop cooling system similar to one the machine's battery has. This helps to keep the cooling liquid inlet temperature and thus converter's temperature lower, but the additional cooling system requires yet again more space. As the machine is operated in sub-zero temperatures the use of glycol as anti-freeze substance in the cooling system in 1:1 ratio with water must be taken into consideration when calculating the required flow rate.

The truck and the converter mounted on it are operated in a rough and uneven terrain where heavy boulders are loaded on the truck so good shock and vibration handling capabilities are required. This must be taken into consideration both when choosing components and designing the mounting of them so that vibrations cannot break the components themselves or damage their mountings and cause a catastrophic failure such as a short circuit within the converter.

Corrosive gasses or liquids that may be present inside the mine for example in salt mines affect the material choices and the outer enclosure must be able to withstand these. Black iron cannot withstand this kind of environment, but stainless steel is preferably used.

The size of the converter is also a key factor for a suitable solution. As the MT42 Trolley is built using an already existing battery powered truck as a base and it has not been originally designed for such additional equipment in mind, the space on the truck available for these components is somewhat limited. Space for the converter and other components is mostly achieved by changing the battery pack to a smaller one as that large capacity is not required anymore to operate the machine efficiently. In the case of the MT42 the size freed by changing the battery to a smaller one is approximately $2170 \times 1580 \times 550$ mm³ resulting in total volume of roughly 1.89 m³. For smaller and larger machines, the available space will be different.

The weight of the converter is an important requirement. Even though these machines weigh dozens of tonnes, the overweight could also affect the dimensioning of the brake systems and it will also have a negative effect on the efficiency of the overall system. As the main purpose of the truck is to transport payload out of the mine and the heavier the truck itself is the less payload can be loaded on to it. Hence the lighter the machine itself is the more payload can be loaded on and the more effective and profitable the machine becomes. Profitability after all is one of the key figures when comparing a machine against other machines or ways of transporting material and estimating its effectivity. The converter and all other additional equipment should not exceed the weight saved by reducing the battery pack and if more weight can be reduced, the better. This means that this additional equipment should have mass less than approximately 1200 kg in case of MT42.

3.1.2 Electrical requirements

The main requirement for the converter is obviously to convert the OCS voltage to the level suitable for the truck's DC-link. Epiroc and other parties in the project want to keep the system voltage within the low voltage directive which limits the nominal input voltage to 1.5 kVDC. As the input voltage supplied by the OCS can vary depending on the load on the OCL segment, the converter should be able to provide the required power ideally also with lower input voltages. It is agreed within the project partners that 900 VDC is kept as the lowest voltage level at which the converter must provide full power and if the voltage drops below this level the power must be decreased linearly until the input voltage reaches 840 V at which point the power is reduced to 0 W according to the railway standard applied by the substation provider. It is beneficial to keep input voltage as high as possible in order to reach the same power with a smaller current. This allows to use lesser copper also in the converter which helps improving its power density and specific power. The secondary side voltage is determined by the VCB battery voltage which varies roughly between 600 – 800 V depending on the state of charge (SoC) of the battery.

The VCB battery is connected directly to the DC-link and the converter's output stage and because of this the converter must be well regulated to protect the battery from possible overvoltage and overcurrent the converter can introduce to the DC-link. The battery is a lithium-ion (Li-Ion) based battery which uses Lithium-Nickel-Manganese-Cobalt-Oxide (NMC) chemistry cells. Like all lithium batteries also this battery's charging sequence consists of constant current (CC) and constant voltage (CV) modes shown in Figure 15 depending on the battery's SoC. In Figure 15 U_{ref} is the battery's full charge voltage typically 4.20 V / cell, I_{ref} is the battery's constant charge current typically ranging between 0.5 - 1 C and I_{CO} is the cut-off current at which the charging is ended typically around 0.1 – 0.05 C, where C is C-rate used to describe battery's current handling capabilities. (Rachid et al, 2018, p. 76)

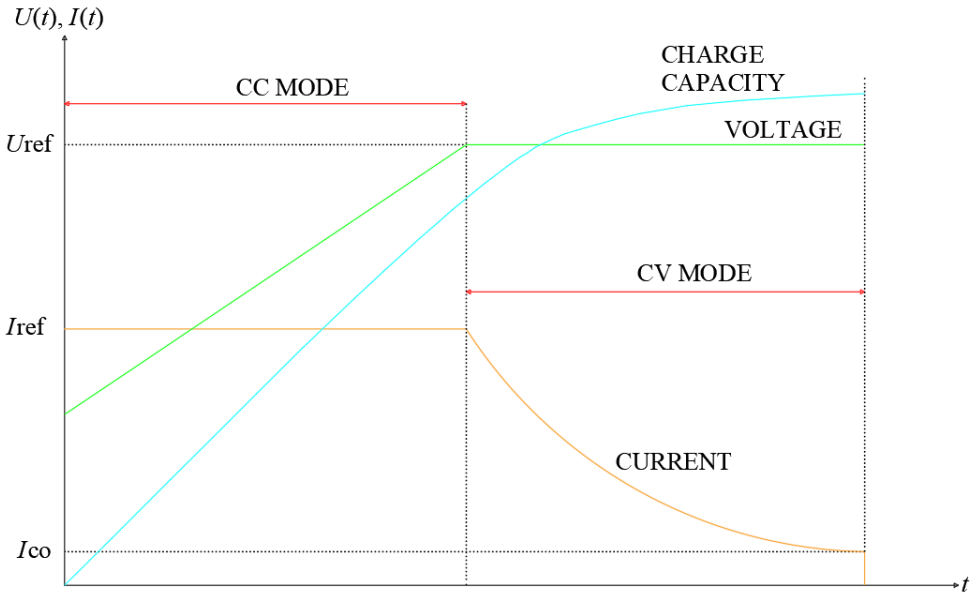

Figure 15.Lithium-Ion battery charge sequence (adapted from Rachid, Fadil & Giri, 2018).

This means that the converter should be able to be operated in either current or voltage regulating modes depending on the SoC of the battery or in other words, its output voltage should follow the DC-link voltage and the output power is controlled by controlling the output current.

The second clear requirement for the converter is its output power. The converter must be able to output at minimum the power the truck consumes while driving up the ramp to unload its dump box on the surface. In addition to the power required by the traction motors some reserve power must be accounted for charging the truck's battery if necessary. In case of MT42 Trolley, the truck's power demand while driving uphill is roughly 450 kW and extra 150 kW is spared for auxiliary systems and charging resulting in total output power requirement of 600 kW suggested by simulations and verified by data gathered with MT42 Battery currently used in the same mine. The current collector solution selected for the first unit sets the maximum input current level to 500 A which results in maximum input power of 450 – 750 kW for the given input voltage range of 900 – 1500 VDC, thus acting as a bottleneck for the system at lower input voltage levels.

Since the trolley solution is later intended to be used also with smaller and larger sized machines which require output power ranging from roughly 400 kW to 1 MW, the easy

scalability of the converter solution is beneficial whereas a unique solution for a certain machine that cannot be easily realised for other power levels is not ideal. In other words, some sort of modularity of the system is a great advantage when considering the solution in longer term. It should be noted that either a different current collector solution or increased input voltage level is needed in future to match the required output power demand.

As the converter is intended to be cooled by connecting it to an existing liquid cooling system of the machine which has not been originally designed to handle such additional losses and only has a certain amount of cooling capacity left, the losses the converter can produce must be limited to this level. The available cooling capacity is not calculated precisely in this thesis, but to give a ballpark number it can be said that the existing cooling system of MT42 Battery could handle 50 kW worth of additional losses without fear of rising the coolant temperature too much. If the losses become too high for the existing cooling system to handle, either the efficiency of the converter must be improved, the cooling system of the vehicle must be improved or as a final resort a separate cooling circuit must be added for the converter as mentioned in the earlier chapter as mentioned while describing the mechanical requirements in previous chapter.

Even though the amount of losses is the determining factor, it is easier to compare the efficiency of different systems and technologies against one another by using the efficiency of the converter rather than the amount of losses especially if the input power of different solutions are not the same. The efficiency η is a ratio of output P_{out} and input power P_{in}, and it can be defined by

$$\eta = \frac{P_{\text{out}}}{P_{\text{in}}} \tag{11}$$

In general, the efficiency of the converter can be improved by using components with low losses and utilizing a control method which enables soft switching. Converter topology has an effect on the efficiency and ease of soft switching as discussed in earlier chapters. Also, as high efficiency as possible is to be pursued to reduce the size of the cooling system and keep the system operational also under high load in high ambient temperature conditions. Smaller cooling solution also improves the power density. With required output power and maximum losses the cooling system could handle it can be roughly calculated that the efficiency of the converter should be higher than 92.3%.

While it is not a strict requirement to realize the design by using SiC-components, utilising those effectively will be seen as a benefit as they enable the use of higher switching frequencies as described in earlier chapters. Higher switching frequency then again allows using smaller magnetic components as explained in earlier chapter thus increasing the specific power and power density of the converter.

As already mentioned, while defining the mechanical requirements, the altitude of the operating environment affects the isolation strength of the air which again in addition to the voltage level and pollution degree determines the required clearance and creepage distances according to the applicable standards.

The electrical system of the base truck is built for the voltage level of 1 kVDC as both the battery pack voltage and the voltage caused by back-electromotive force (EMF) while regenerative braking are well below this limit. This level is realised with the selected components used within the DC-link ranging from used connectors to the traction inverters et cetera. Because the machine is to be coupled to the OCS which voltage could be as high as 1.5 kVDC, the converter must be an isolating one meaning that there is no galvanic connection between its primary and secondary stages. Isolated converter is required to protect the machine's DC-link from OCL voltage as failures in the converter could potentially lead to a break-down of the insulation somewhere in the machine's DC-link. Strong enough isolation strength between the primary and secondary stages as well as these stages and the chassis are required so that even the quick transients cannot cause issues during the lifetime of the machine.

The isolation between the primary and secondary stages of the converter is helpful also to prevent insulation monitoring systems within the machine's DC-link and OCS from disturbing each other. If the converter were not isolating, these two insulation monitoring systems would be practically connected in parallel to each other which would cause interferences.

While the bidirectional power flow is not a strict requirement, it for sure is helpful. Converter must have an input stage which filters the interruptions in the power supply caused by intermittent connection between the current collector's contact strips and the OCL and provides compatibility with the OCS. This filter consists essentially of inductors and a capacitor bank. If this capacitor bank is connected directly to the OCS when it is fully

discharged, there is a risk that the inrush current caused by charging this capacitance will trip the overcurrent protection of the converter input. To prevent this, a bidirectional converter can be utilized to pre-charge the capacitors to the same voltage level than the OCS is at so no harmful inrush current will be present during the connection. Another way to handle the pre-charging would require an additional pre-charging circuit, consisting of a resistor and a contactor, which is connected in parallel to the main contactor. In practice, it would be used so that the initial connection is made through the pre-charging circuit which effectively limits the inrush current to a level that can be handled by the input over current protection. With this solution the bidirectionality is not required but a simpler unidirectional converter can be used instead.

During the downhill drive back to the mine, that can take even half an hour, the bidirectional converter could be used also to transfer energy from the truck back to the OCS. This would be beneficial since energy regenerated with one truck while driving downhill could be transferred to the OCS and utilized with another truck that is driving uphill at the same time. If another truck is not driving uphill simultaneously the energy could be stored in a decentralized energy storage such as a battery pack, utilized in some other way, fed back to the grid or in a the most inefficient case consumed in a brake resistor. Some of the energy can be stored in the truck's own battery pack but this capacity is limited due to the relatively small size on the battery mounted on the vehicle. A brake resistor on the truck is also an option but it requires a large volume and efficient cooling. So, moving these out of the vehicle to the mine, where space is not an issue and the system can be decentralized, could help solving many potential problems.

The reliability of the machines is a priority in this industry. Due to the hostile environment in which these machines are operated, long operating hours per day and application which puts high stress on every single component of the machine, the lifetime of these machines can be as short as five years. It is therefore not feasible to design the converter with 20-year lifetime as it results in too large margins and over dimensioning of the system. Mean time between failure (MTBF) however should be as long as possible as in the worst case a single fault in the converter may cripple the functionality of the whole machine. Mazumdar et al. (2010, p. 1158–1165) suggest in their study a MTBF value of 24 months for the whole machine and Epiroc has typically defined a value of 24000 hours which corresponds to MTBF of roughly 50 months calculated with 16-hour operating time per day. Modular

design consisting of multiple parallel connected modules can increase the redundancy thus improving the usability during a single converter module failure.

3.2 Market study

One part of this thesis is to conduct market research to find out if suitable converters for the trolley truck application do exist on the market and then determine which one of these converters would be the best fit for Epiroc's use case. This market study is conducted by first searching for converter manufacturers who have specialized in such high voltage and power levels and then comparing their actual products and concepts with each other. The main part of the market study was conducted between Q3 2021 and Q2 2022 by first doing research on the internet then contacting possible manufacturers and finally having meetings with them to learn more about their company and their products. Discussions with a few manufacturers whose products were the most promising were continued for a longer period of time while others were met only once or twice. Hence, there are differences in the number of details in each of the solutions.

Approximately ten different manufacturers were found during the market search and five most promising solutions from these manufacturers are presented in the following sub-chapters. All the solutions are from different manufacturers. The name of the manufacturers is not revealed but they are simply referred to as solution A, B, C, et cetera.

3.2.1 Solution A

The solution A from is based on a product series its manufacturer has developed originally for a railway application in which it is intended to be used as a bidirectional converter between the energy storage system (ESS) of the train and the high voltage DC-link for traction motors. The converter for Epiroc is based on this same design but some the some of the electrical, and first of all, the whole mechanical interfaces have been adapted to be suitable for the MT42 Trolley instead of a train. The solution A is built out of two parallel-connected converter modules and an input stage shown in Figure 16.

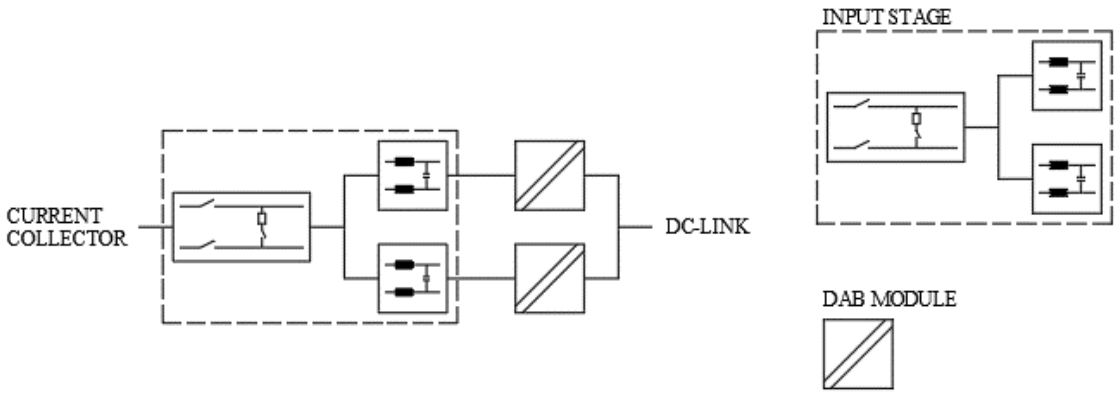

Figure 16. Solution A: basic construction.

Figure 17 illustrates the basic construction of a single converter module of solution A. It utilizes DAB topology which makes it isolating and bidirectional. Each of the two modules has two parallel-connected primary stages built out of series connected H-bridges to improve the current and voltage handling capabilities of the converter. Each module has one transformer per H-bridge resulting in total of four transformers. These transformers are grouped in pairs that share common core as shown in Figure 17. Secondary windings of each transformer pair are connected to their respective secondary stage H-bridges that are connected in parallel. Converter is built using traditional Si IGBTs as switches and designed so that it can operate at a wide range of input voltage ranging from 840 VDC all the way up to 1800 VDC and the maximum power it can output is 800 kW. Output power varies depending on the input and output voltages and in practice, the available power varies between 340 kW at 840 VDC input voltage and 560 kW at 1500 VDC input voltage which has been set as the maximum output power in case of MT42 Trolley.

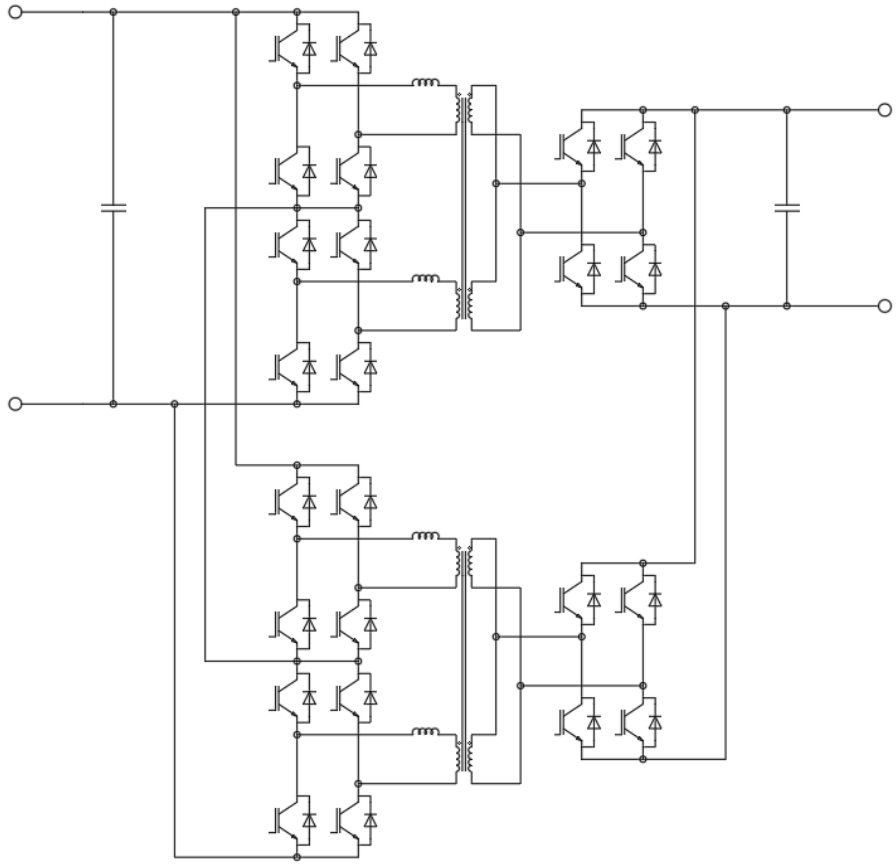

Figure 17. Solution A: single module schematics.

The converter is controlled with manufacturer's self-designed centralized controller. The main control interface between the vehicle and the controller is Control Area Network (CAN) bus which utilises SAE J1939 protocol typically used in different kinds of vehicle applications. The controller provides also digital inputs (DI) and outputs (DO) as well as analogue inputs (AI) and outputs (AO) for different internal and external interfaces such as current and voltage measurement signals for the feedback loops, temperature measurement of different parts of the system as well as some galvanically isolated DI and DO interfaces between the controller and the vehicle for the safety critical signals. Same controller oversees the controlling the modulation of the switching stages. Controller has an opto-isolated interfaces with each of the gate drivers of the IGBTs which it uses to command each IGBT according to the modulation scheme and to receive state and fault messages from the gate driver. The converter is modulating using triangular modulation which enables ZCS leading to reduced switching losses. According to the manufacturer the efficiency of the solution A

is roughly 94.4 – 95.6% depending on the operating point. Switching frequency of solution A is 4 kHz which is rather typical for an IGBT based high power converter.

In addition to the converter modules, other additional parts of the trolley system are built into the same cabinet. The largest of these are main the contactors required for electrically separating the current collector from the input of the converter, cooling fans and heat exchanger circulating the air inside the cabinet and transferring heat to the cooling liquid as well as the input filter required for smoothing the input voltage to the converter due to the intermittent connection between the OCL and the current collector. This input filter consists of a capacitor bank as well as smoothing reactors which are symmetrically distributed to both parallel converter modules.

In order to fit the converter to the MT42 Trolley it has been built into a custom-made steel frame which provides IP65 rated ingress protection and necessary interfaces for mounting, voltage class A and B (VCA and VCB respectively) connections and liquid cooling. The dimensions of this custom-made enclosure populate the whole volume freed by the reduced battery pack resulting in total volume of 1,5 m^3.

The converter is cooled with liquid cooling circulation which is provided by the vehicle. Switching stages are mounted on a cooling block which allows efficient cooling of the power electronic components. Also smoothing reactors of the input filter are connected to the same liquid cooling loop. Other components producing losses as heat such as transformers are cooled with forced air cooling by circulating air inside the cabinet with a cooling fan. A heat exchanger is then used to transfer the heat from the air into a cooling liquid.

3.2.2 Solution B

The solution B is based a combination of two different types of converters the manufacturer has developed earlier for their other customers. It consists of a series connected isolating resonant converter and a bidirectional converter topology that is capable to step-up and step-down the input voltage. The exact topologies are not disclosed in this thesis, and they are referred to just as resonant converter and buck-boost converter. Manufacturer has existing products that utilize these topologies, but cascaded converters built in a common enclosure must be designed. The manufacturer has also earlier experience of a similar operating

environment as one of their products has been designed for and is already used in an off-highway application. Solution B was found outside the market study conducted for this thesis and the author has not taken part in the discussions with the manufacturer, so the information presented in this thesis about the solution is somewhat limited.

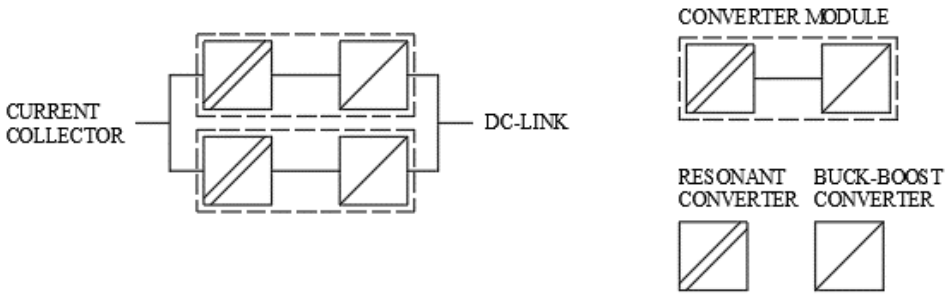

Figure 18. Solution B: basic construction.

The solution B is capable of converting voltages between 0 - 2.4 kV bidirectionally with a maximum current capability of 400 A or power capability of 500 kW, so in order to fulfil Epiroc's power requirements for MT42 Trolley also with lower input voltages, two of these modules are connected in parallel. According to the manufacturer up to 16 of these modules could be connected in parallel. So, the system is modular, and it would therefore be suitable to cover Epiroc's whole machine portfolio easily.

The buck-boost converter utilized in solution B has originally been designed for a NRMM application which utilizes fuel cells as an energy source. The said converter's first generation is already on the market and an improved second generation was released for production during the end of the year 2022. The isolation for the solution B is realised by using a series connected fixed ratio (1:1) resonant converter whose output voltage follows its input voltage, and its task is just to provide isolation. At the time of the writing this thesis (Spring 2023) the manufacturer is unsure if they can utilize the existing isolation stage as it is or if they need to make some modifications to it.

Manufacturer intends to use a planar PCB coiled transformer for the isolating stage, with the design they have patented. According to them, it allows optimized volume and efficiency regardless of the high currents and frequencies while skin effects and proximity effects are mitigated efficiently. They also say that the PCB windings offer great repeatability from a

manufacturing point of view and strong insulation which are beneficial when designing such high voltage systems. Lastly, they assure that the said design is suitable for the intended harsh environment and has been tested against military aviation standards for vibrations and thermal shocks.

Solution B utilises soft switching for both converters. On the resonant converter's primary side all the switching operations are ZVS and on the secondary side all the switching operations are ZCS which reduces the switching losses effectively. Judging from the high efficiency of the buck-boost converter, it utilizes also some type of soft switching. The manufacturer estimates that the efficiency of the isolation stage could be as high as 99.5% and the efficiency of the buck-boost converter could be 98.5% resulting in a total efficiency of approximately 98.0%.

Solution B is liquid cooled and relies on external heat exchanger provided from the vehicle side. Total efficiency this high means that the vehicle's existing cooling system could easily handle the additional losses from the converters without any modifications. Small thermal losses also mean that the solution could more easily be used in a higher ambient temperature of mines located in the southern hemisphere where temperatures underground could be tens of degrees higher than what we are accustomed to here in Northern Europe.

Since the manufacturer's roots are in mobile applications where the size and weight of the converter must be squeezed to as small as possible, all of their designs are based on WBG technology. The solution for Epiroc has been built using SiC MOSFETs as switches which allows it to use really high switching frequencies up to 300 kHz which allows the magnetic components to be really small resulting in a very compact and power dense system.

The manufacturer believes that there is no need for an input filter as their converter can handle very disrupted input voltage waveforms, so they have left it out from their design offering only the converters as stand-alone modules. There also is no mention of a main contactors, external protective circuitry nor interconnection of the modules and therefore the possible components for the infeed circuit et cetera are to be added externally to the converter solution possibly by Epiroc and add the weight, size, and cost to some degree.

The control system of solution B is not completely revealed in the provided material, but it appears to be a distributed system where each converter has its own controller which the machine's control system is communicating with. This communication seems to be based

mostly on the CAN-bus and only some hard-wired digital signals for enabling the converter need to be provided.

Solution B is built into an enclosure milled out of aluminium and it provides IP67 protection for the module. Interface for the VCB connections is not fully settled and therefore it is not clear if it provides sufficient ingress protection or if additional enclosure is required around the modules. As mentioned earlier, both the isolating resonant converter and the buck-boost converter are built into a common enclosure forming one module and the total system consists of two of these modules. Each module has interfaces for the input and output power cables, cooling liquid manifolds and a signal cable connector. All the components inside the converter are mounted so that they can handle shocks and vibrations well. With such a tightly packed system capable of handling voltages up to a few kilovolts it is crucial that not even high mechanical shocks can result in a failure of mounting components, or the results could be catastrophic as short circuits might cause even a fire.

3.2.3 Solution C

Solution C consists of two converters connected in series, a buck converter and a full-bridge converter. Solution is built using parallel connected modules and each one of those has a nominal power of 50 kW. For MT42 Trolley 12 of these modules are to be connected in parallel resulting in total power of 600 kW as shown in Figure 19.

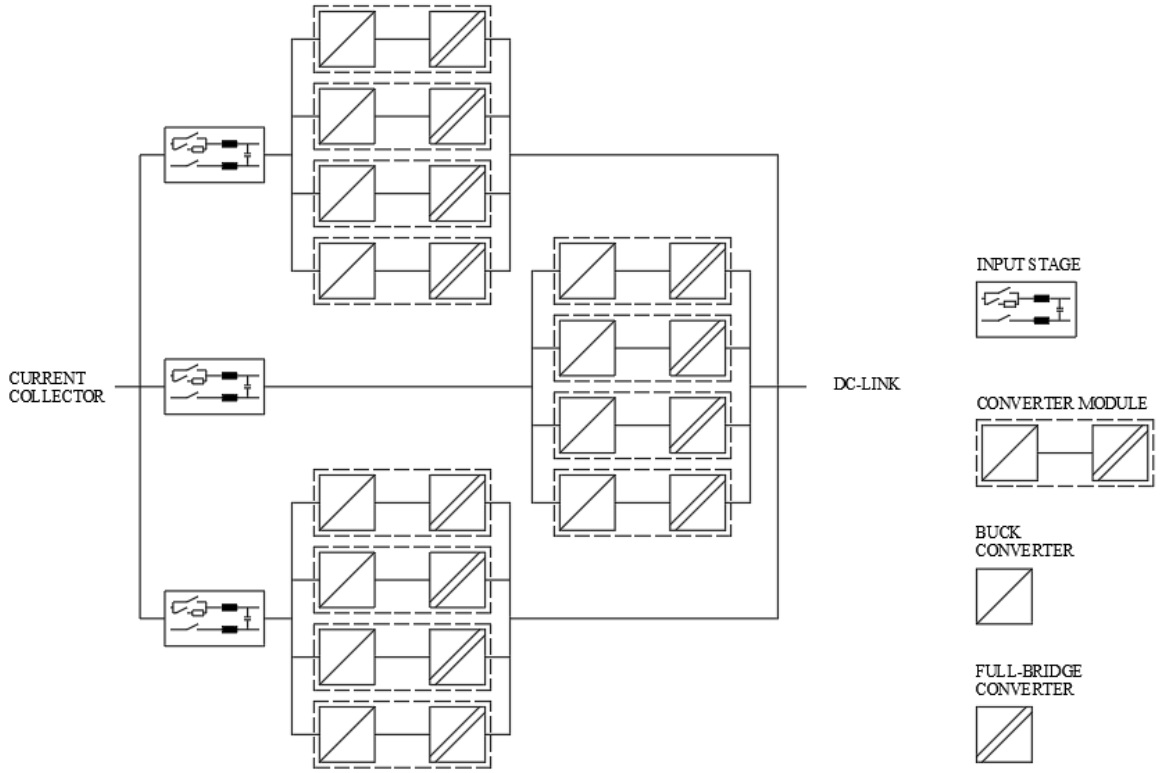

Figure 19. Solution C: basic construction.

The manufacturer tries to apply the existing design as much as possible, so the full bridge converter design is taken from an earlier project as it is, but since it has been developed for a lower input voltage level a simple buck converter and a gate driver for it are designed and connected in front of it to step down the OCL voltage to an appropriate level of 900 V as shown in Figure 20.

The buck converter is built using a module consisting of a 3.3 kV Si IGBT and a diode which allows its footprint to be smaller. Its purpose is simply to step down the OCL voltage of up to 1.5kV to a lower level of approximately 900 V so that there is enough voltage margin for the SiC MOSFETs of the full-bridge converter's input stage. The full-bridge converter has a single H-bridge on its primary stage and two parallel connected transformers and output stages. Switching stages are built using SiC technology. On the primary side 1.7 or 1.2 kV SiC MOSFETs and on the secondary side 1.2 kV SiC diodes are used. Use of diodes on the secondary side make the secondary stage act as a passive rectifier which does not need to be actively controlled and is capable to only unidirectional power flow as described in earlier chapters. Even though this makes the converter design more straightforward, an additional pre-charging circuit such as described while defining electrical requirements is required.

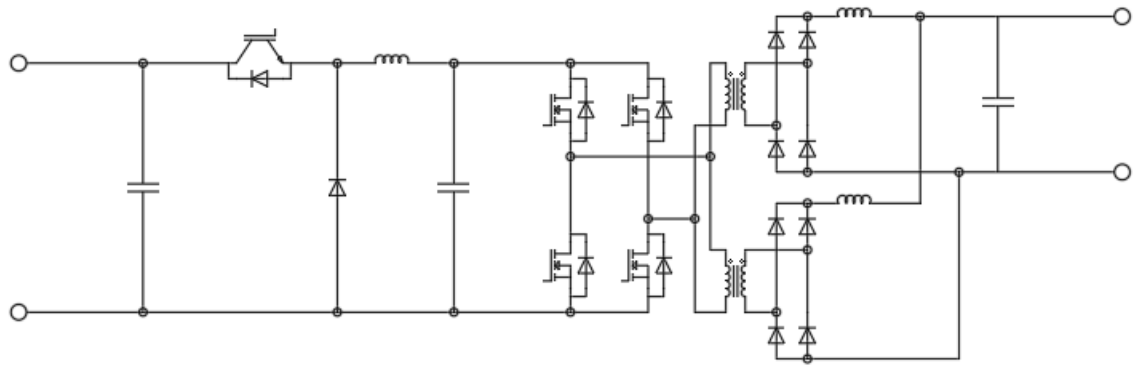

Figure 20. Solution C: single module schematics.

In late 2021 as the whole world was still suffering from the global supply chain difficulties caused by the pandemic the manufacturer of solution C suggested to use Si IGBT technology for the buck converter as it was proven to be a robust solution in such an application, and it was easily available at the moment. SiC technology was also on the market but the lead times were really long and most of the retailers did not have them in stock in larger quantities. During the concept design the availability of SiC technology however has improved and therefore the manufacturer now believes that the buck converter could be built also by using series connected SiC MOSFETs or the need for it could be even totally eliminated by implementing such design of series connected switches for the main full-bridge converter. This would most likely have a positive effect on the efficiency of the buck converter and marginal effect on the size of the converter module. However, for the concept covered in this thesis as solution C, Si-based buck converter design is considered as that has been the base for the discussions and concept.

The switching frequency used in solution C is 10 kHz which is relatively low for a SiC based switches. Both the buck converter and the full-bridge converter utilize hard switching which according to the manufacturer gives low enough losses from a technoeconomic perspective so that soft switching is not required when the design is realised with SiC switches. Even though SiC MOSFETs are not used to their fullest potential what it comes to switching speeds and mitigating losses, using those enable the use of higher switching frequencies when compared to Si based system, which is beneficial for the size of the converter. Manufacturer states that hard switching allows them to keep the overall design of the

converter simpler as no additional resonance circuits to realise the soft switching are required. The manufacturer has calculated that each of the converter modules produce 2.1 kW losses and input filter reactances produce 2.0 kW at full 50 kW output power. The efficiency of a single converter module is then 96.0% and with the MT42 Trolley's 12 converter modules and 3 input filters the total system losses and efficiency are 31.2 kW and 95.1% respectively.

Control interface concept between the vehicle and the converter is not strictly defined at the moment and the manufacturer has suggested different approaches, one centralized and one distributed control system. The manufacturer tells that they typically use hard wired signals to control the converter's main functions and CAN-bus messages are used only for other "nice to have" messages that are not safety or time critical due to the reduced latency and improved reliability of the hard-wired interface. They are also able to realize the controller with safety rated control up to safety integrity level 2 (SIL2), which would require a hard-wired control interface. The latest control concept is such that each converter module has an internal control board which can control the switching actions of each converter based on the hard-wired signals it receives from a PLC or machine's control system. The said PLC would also act as a gateway for the CAN-bus between the machine and the converter system. The manufacturer has however stated that the whole interface could be based on CAN-bus if Epiroc wishes so.

Both converters are built in a common enclosure which forms a single module. The manufacturer has made a concept of the converter module where each module has approximately 40 l volume and 30 kg mass. A converter module can then be lifted out easily by hand if a need emerges for example during maintenance. Each module has connections for input and output power cables, low voltage power and control interfaces and input and output cooling liquid connections so that they can be connected inside the enclosure. A large liquid cooling block in the middle of the module divides the module in two and all the components that require cooling are mounted on both sides of it. A sheet metal cover is built around the module but is not waterproof and it only offers basic touch protection, so an external cabinet is needed to protect the modules from mine contaminants.

In addition to the converter modules the manufacturer has taken into consideration the input filtering stage, input contactors and over current protection which are in their concept considered to be common per few converter modules as shown in Figure 19. Even though

this requires a larger number of components than one common input stage for the whole solutions, it allows smaller rated components to be used which tend to be smaller in size. With such approach the modularity can be better utilized to a greater potential. If one converter module was to become faulty only that group of converter modules would need to be switched off and disconnected and the rest of the system could be used just as before the fault with reduced total power. Whereas with just one large converter the whole system could be useless in case of just a single fault.

Mechanical concept of solution C includes a single cabinet to which all the modules, infeed circuitry and cooling piping are placed in similar to solution A. However, the mechanical design of the cabinet has only been presented as a basic concept and more detailed design has not been currently done. The manufacturer doesn't capabilities to design nor manufacture the cabinet so those tasks would probably fall on Epiroc or some third party.

3.2.4 Solution D

Solution D is based on an existing topology which is scaled upwards. It is built using a two-switch flyback topology which makes it isolating and unidirectional. The design is realised using SiC-based switches which allows the converter to have a switching frequency of 60-90 kHz. Due to the high switching frequency and soft switching the manufacturer believes they can reach efficiency level of 96-98 %. Converter could accept voltages up to 1.5 kV and convert it to correct battery voltage level of the machine.

Solution D relies on dozens of parallel connected converter stages to achieve the specified total power like shown in Figure 21. According to the manufacturer the total number of the parallel connected converter stages would depend on the efficiency of the cooling system the vehicle has to offer but the manufacturer estimates that up to 40-50 stages would be required to achieve the 600 kW total power.

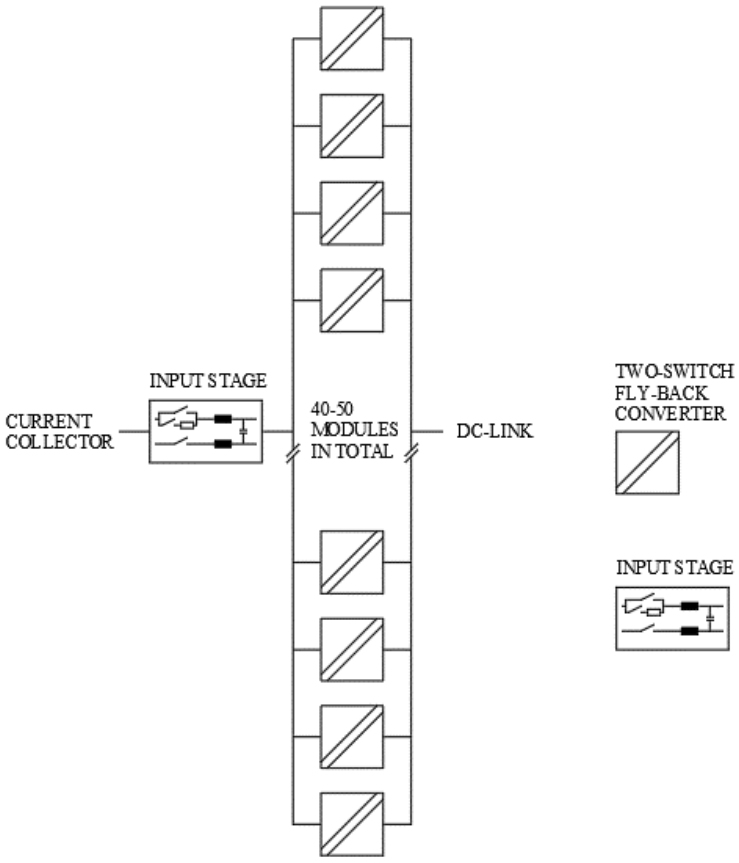

Figure 21. Solution D: basic construction.

Manufacturer plans to assemble the solution D into a suitable sized off-the-shelf Nema 4 rated cabinet built of stainless steel which would offer IP67 rated protection for the converter. In addition to the converter modules also input filter and a pre-charging circuitry are placed in the same cabinet. Manufacturer cannot specify the exact size of the converter at this state but is confident that everything could be fit into the given space.

3.2.5 Solution E

The manufacturer offers a solution based on one of their off-the-shelf products as solution E. Even though it is not a catalogue product it is something similar they have developed as a custom product before and hence they believe it would be easily implemented again. Solution E is a modular converter utilizing an isolated buck-boost converter topology and WBG technology. It consists of parallel connected converter modules, each of which would be capable of producing roughly 60 – 80 kW, so eight to ten of these modules would be

required to would be required to achieve the power of 600 kW for MT42 Trolley like shown in Figure 22. The efficiency of the converter is 90-98 % depending on the operating conditions. The converter is controlled with CAN interface.

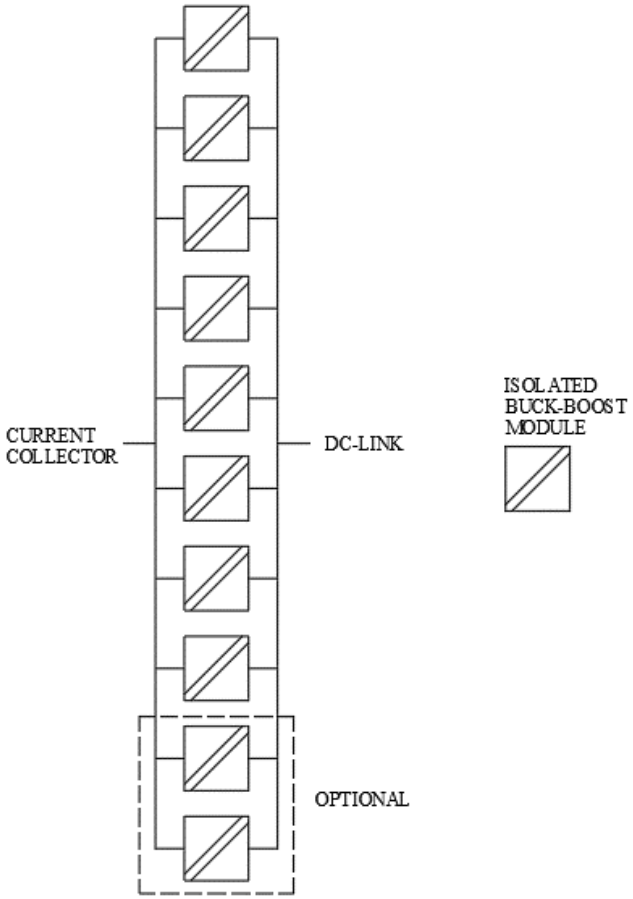

Figure 22. Solution E: basic construction.

Each converter module is built into a stainless-steel enclosure which offers IP65 rated protection against the elements and has necessary connection interfaces for VCA and VCB supplies, control and liquid cooling. A single module would have around 20 – 30 kg mass and its volume would be roughly 25 l. Without possible input filter, mounting frame and other additional parts the size of the total system would then be roughly 300 kg and 250 l.

The most critical downside of the solution E is that its maximum input voltage is only 950 VDC which would result in too high amperage for the rest of the trolley solution's components such as the current collector with the given power. The manufacturer estimates

the engineering cost of a solution capable to withstand higher input voltages so expensive that negotiations for a more customized solution are not continued.

3.3 Comparison of different solutions on the market

Out of the five most promising manufacturers and converters presented in the previous chapter, the top three, solutions A, B and C, are compared in this chapter. Different areas of these solutions are presented side by side and then compared against the set requirements and each other. The remaining two converters presented in earlier chapters but left out of the comparison have some good characteristics but due to their unsuitable properties or immature state they cannot be considered for this application and are hence left out of this comparison.

3.3.1 General concept and electrical properties

Comparison is started by looking at the general concept and electrical properties of different solutions and an overview of each these for each solution is given in Table 2. Solution A relies on a DAB topology which in combination with high-voltage-rated IGBT switches allows it to be used on its own. DAB converter provides required isolation and also bidirectionality which is not an absolute requirement but a preferred property. Solutions B and C share the common idea of two series connected converters, but the similarities of the topologies end there. Solution B has a Resonant converter with 1:1 conversion rate and its purpose is solely to function as an isolation stage while the series connected bidirectional buck-boost converter provides the voltage conversion. Solution B is built using SiC MOSFETs and even though the type of these is not known the voltage range of the converter suggests either three 1.2 kV or two 1.7 kV rated SiC MOSFETs are connected in series. Solution C has a full-bridge converter which handles the conversion and isolation but since it has originally been designed for another application in which such high input voltage was not needed it needs to have a buck converter connected prior to it in series to step down the voltage. Buck converter is built with a 3.3 kV Si IGBT and a full-bridge converter with 1.2 or 1.7 kV SiC MOSFETs on its primary side and 1.2 kV diodes on the secondary side which does not allow it to be used bidirectionally.

The number of parallel connected converter stages and modules and overall number of cabinets are presented in Table 2. There are no requirements from Epiroc regarding these, but it nonetheless presented as it gives an idea on how each solution is built, what kind of components are used in it and how modular it is. Solution A has one cabinet in which two parallel connected converter modules are housed. Each of these two modules has two parallel connected converter stages resulting in total of four parallel connected stages. Solution B has two parallel connected modules, but at the moment of writing the thesis the concept does not state if these modules are built into a common cabinet or if those are mounted directly on a frame. Each module has one resonant converter and in series with it four parallel connected buck-boost converter stages. Solution C has 12 parallel connected converter stages each consisting of a series connected buck converter and a full bridge converter. Each stage is built into its own module and all the modules are assembled in a common cabinet.

Table 2. Comparison of general concept and electrical properties.

	Solution A	Solution B	Solution C	Requirement
Topology	DAB	Resonant + Buck-Boost	Buck + Full-bridge	NA
Technology	Si IGBT	SiC MOSFET	Si IGBT, SiC MOSFET and SiC diodes	SiC preferred
Isolating	Yes	Yes	Yes	Yes
Bidirectional	Yes	Yes	No	Preferred
Number of parallel converter -cabinets -modules -stages (total)	 1 2 4	 ? 2 2+8	 1 12 12+12	 NA NA NA
Output power -per module [kW] -total [kW]	 400 800	 500 1000	 50 600	 NA 600
Input voltage -Typical [VDC] -Max [VDC]	 840…1500 1800	 0…2400	 840…1500 1900	 840…1500
Output voltage [VDC]	600…800	0…2400	600…800	600…800

Switching frequency [kHz]	4	300	~10	NA
Switching method	Soft switched ZCS	Soft switched ZCS & ZVS	Hard switched	Soft switched preferred
Efficiency [%]	94.4…95.6	< 98.0	95.1	> 92,3
Losses @600 kW [kW]	35.6	12.2	31.2	~50.0

The maximum output power is shown in Table 2 and output and input powers as a function of the input voltage are presented in Figure 23 and Figure 24 respectively. For solutions A, B and C each manufacturer has given either the output power or output current limitation which has been used to calculate the values shown in Figure 23. Then using the efficiency estimation and the calculated output power the input power has been calculated and it is presented in Figure 24. Because manufacturers have reported the efficiency only at one operating point it is considered to be constant for the whole operating range for the sake of simplicity and the lowest announced value for each solution is used. This does not provide fully accurate result as the efficiency does vary depending on the operating point, but it helps describing the operating ranges of each solution. For solution A manufacturer has given two different power values based also on the converter's output voltage, in these figures referred as *Low SoC* and *Full SoC*.

The output power requirement of the converter for MT42 Trolley is 600 kW for input voltage between 900…1500 VDC. Solution A is capable of producing output power up to 800 kW at 1.6 kVDC but it can reach the required power of 600 kW only at rather high voltage of 1250…1390 VDC. This means that it is not likely to be able to provide enough power for both traction motors and for charging the battery if the OCS voltage is at its low end. The manufacturer has defined the power for up to 1.6 kV, but the converter could handle even higher voltages than this. Solution B is capable of producing power up to 1 MW and its voltage range is 0...2.4 kVDC making its output power and input voltage range the best out of these three solutions. Solution C has been designed for the given input voltage range and output power so it can fulfil both these requirements. Output power has been defined up to 1.5 kV, but the converter can handle input voltages up to 1.9 kV.

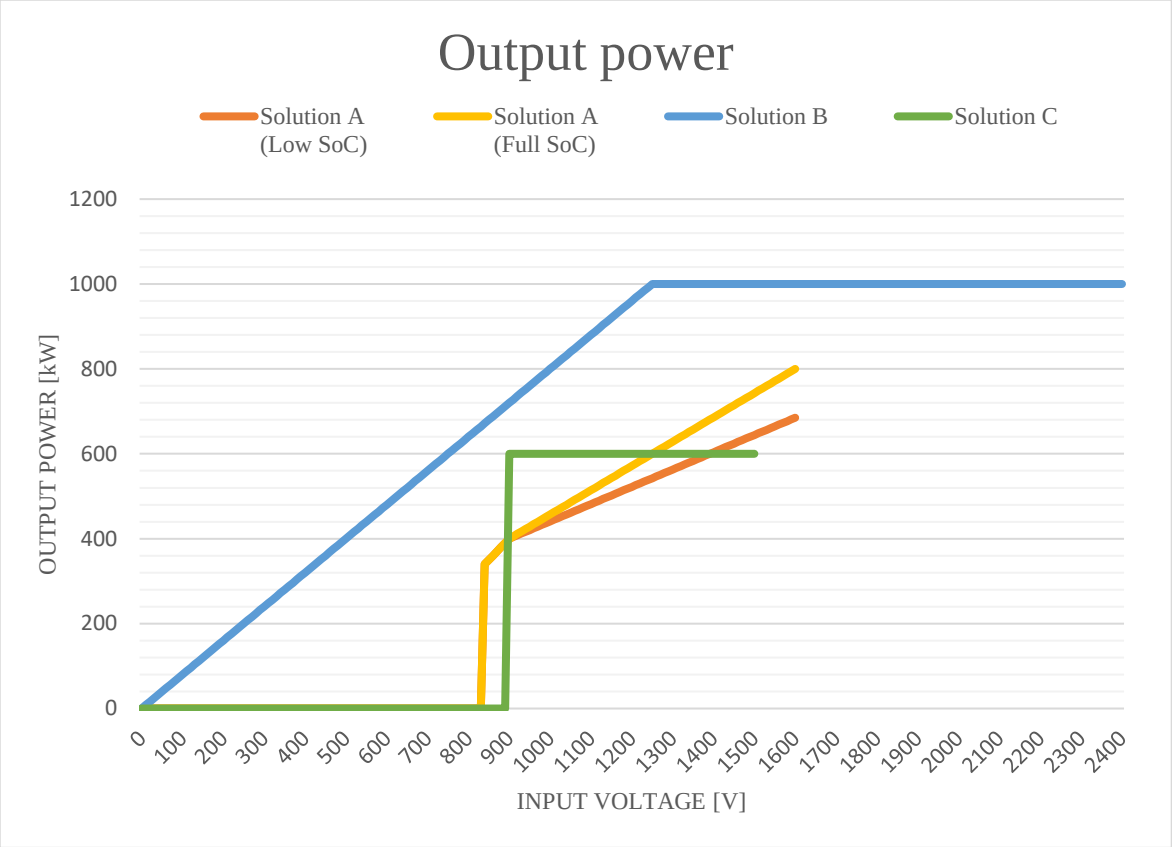

Figure 23. Converter output power as a function of output voltage.

In addition to input power of each solution also maximum current limitation introduced by the current collector is presented in Figure 24. It can be seen that the maximum amperage of 500 A for the current collector indeed limits the available input power so that the required output power of 600 kW can only be reached once the input voltage exceeds 1.2 kV. This is a known restriction that should be fixed with later current collectors. In Figure 24 it can be seen that this restriction affects limits the output power of all other solutions but solution A with low output voltage.

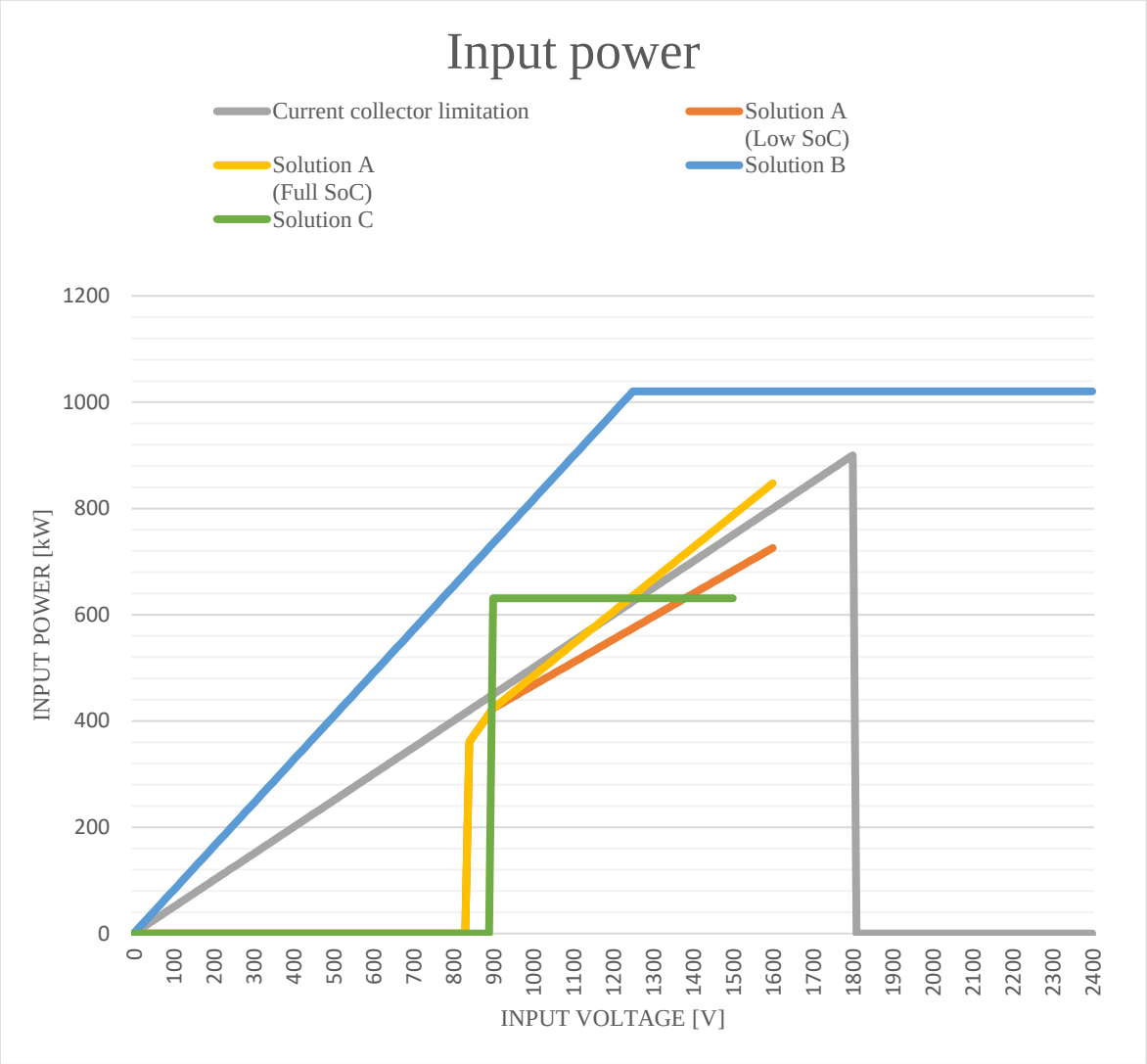

Figure 24. Converter input power as a function of input voltage.

In Table 2 converter switching frequency, switching method and efficiency are considered. Solution A uses IGBTs which are slow to be switched hence resulting in large size as rather large inductances and transformers are needed. Solution A utilizes triangular modulation which allows it to use ZCS which helps it to reduce some losses. The manufacturer has stated the losses of the converter at two output power levels which yields its efficiency to be around 94.4…95.5% at typical operating points. Solution B is built using SiC MOSFETs which allows the use of comparably high switching frequencies. The manufacturer states that as high as 300 kHz switching frequency could be used resulting in 75 times as high switching frequency as in solution A and 30 times as high as solution C. Solution B utilizes ZVS on the primary side and ZCS on the secondary side resulting in greatly reduces switching losses.

The manufacturer states that the efficiency of the resonant converter is up to 99.5% and the efficiency of the buck-boost converter is 98.5% resulting in total efficiency of 98%, which is highest of the three. The switching frequency for solution C is only 10 kHz which is rather low for a converter using SiC MOSFETs. The manufacturer has wanted to increase the switching frequency high enough to make the converter's magnetic components smaller than with IGBT switches would allow but since the converter uses hard switching and it therefore cannot reduce its switching losses the switching frequency is kept at a rather moderate level. Despite hard switching the efficiency of the system is 95.1% placing it on par with solution A. Finally, the given efficiency for each solution is used to calculate the losses at unified 600 kW output power level. All solutions can reach the required efficiency and keep the losses low enough.

Out of these three the modularity of solution A is the worst due to its large size and the fact that its mechanical enclosure has been specifically designed for MT42 Trolley. Even though the converter has potential of being modular since it has been built out of two parallel connected modules it has not been realised to its fullest potential. A complete mechanical redesign of the solution must be made if the system is to be used with larger or smaller machines. Due to small size and high power of the solution B module its modularity is the best. Two module system allows the same solution that is used with MT42 Trolley to be used also with larger machines and for smaller machines another module can be left out completely or if there is space for it, left connected and used to improve the redundancy. Solution C has been designed with the modularity in mind. It has been built out of parallel connected modules and input filters resulting in total of three 200 kW systems. These stacks can be used to form solutions for smaller and larger machines in steps of 200 kW. The frame and mechanical enclosure to which the modules are mounted on must be designed separately for each machine size based on the number of modules required.

3.3.2 Mechanical properties

The mechanical properties of different solutions are compared in Table 3. The dimensions, volume, mass and power density of modules and whole solutions are compared against the requirements given by the machine.

As mentioned in the earlier chapter, the mechanical dimensions of the converter are limited by the space that is freed by reducing the size of machine's battery pack. This size available for the converter in MT42 Trolley is roughly 2170 × 1168 × 550 mm with a small extension resulting in total volume of 1.547 m³. The space is located at the front of the machine between the driver's cabin and the new battery pack.

Table 3. Comparison of mechanical properties.

	Solution A	Solution B	Solution C	Requirement
Size (*L*×*H*×*W*)				
Module [mm]	~1700×1163×530	>700×750×90	420×225×440	
-Total [mm]	2170×1580×530	~1000×1000×250	2160×1168×550	<2170×1168×550
Volume				
-Module [l]	~530	47.3	41.6	
-Total [l]	1491	250 (est.)	1388	< 1394
Mass				
-Module [kg]	NA	45	30	
-Total [kg]	1400	300 (est.)	1000	< 1200
Power density [kW/l]				
-Module:	0.755	10.6	1.22	NA
-Total:	0.537	4.0	0.432	>0.430
Specific power [kW/kg]				
-Module:	NA	11.1	1.67	NA
-Total:	0.571	3.3	0.600	>0.500

Looking at the total dimensions and volumes of each solution, both solutions A and C fill more or less the whole given space. The dimensions of solution B are estimated based on the existing buck-boost converter's design with roughly 50% increase to each dimension. It can be clearly seen that the total size of the solution B is only a fraction of the solutions A and C resulting in clear advantage for solution B.

The mass of module in solution A is not specified but the masses of both solutions B and C are less than 50 kg. Solution C's module mass is the lightest of the three and it has been designed so that it can be lifted even by hand without a crane. Solution B's module mass is slightly heavier 45 kg. When looking at the mass of the total solutions, the mass of solution

A is 1400 kg which exceeds the requirement by 200 kg. Solution C then again is approximated to have mass around 1000 kg which is rather high but still acceptable. The manufacturer of solution B has stated only the mass of a single module, so the total mass of the solution has been estimated to take the casing and other lighter components such as the main contactors, cabling and cooling piping better into account by calculating the mass of steel plates that match the estimated dimensions of the cabinet and adding some margin to. It is estimated that in total this additional mass is roughly 200 kg. The estimation does not take into consideration infeed circuitry that is possibly required and which can add easily one to two hundred kilos worth of mass but even then, the solution B would still be the lightest of the three.

The comparison of the total system volume and mass is not quite fair as different solutions do not have unified output power and the volume and mass estimations of solution B do not take the input filter into account that are considered in solutions A and C. Comparison of power densities and specific powers gives therefore more truthful idea of each solution's performance, even though some of the dimensions and masses are only estimations. The power densities and specific powers of each solution are presented in Figure 25.

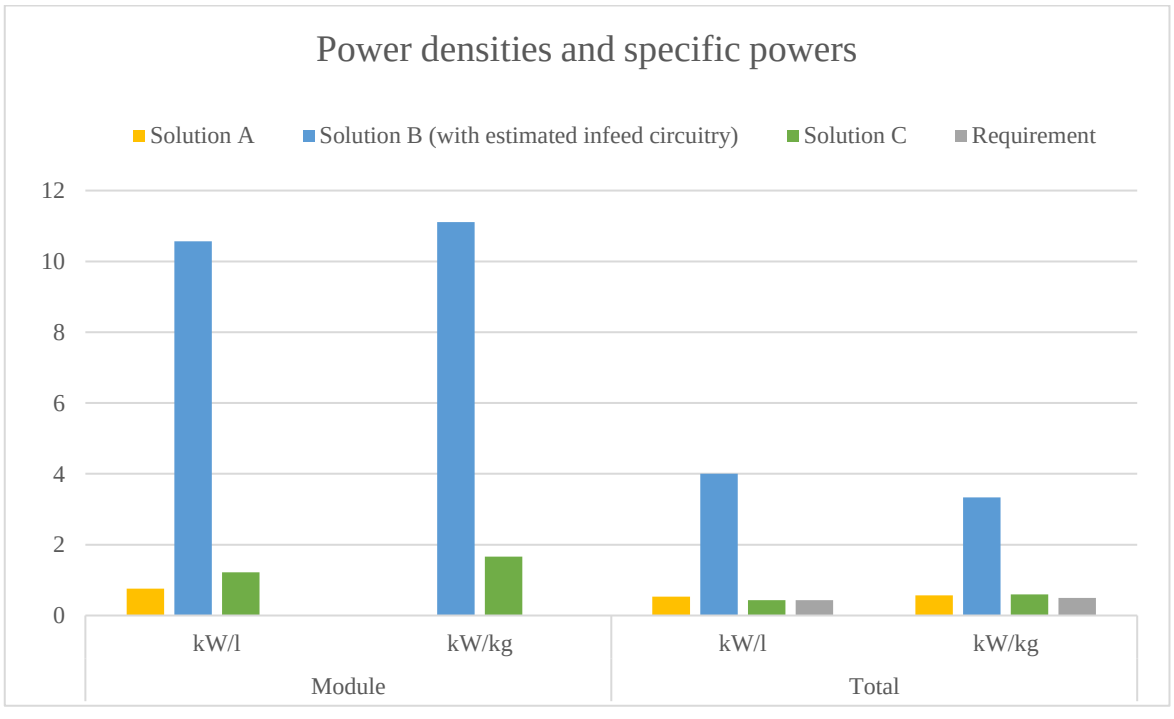

Figure 25. Power densities (kW/l) and specific powers (kW/kg) of different solutions.

This graph quite clearly presents the supremacy of the solution B in this sense as its power density is ten times as high as in solutions A or C on a module level and even though the total system volume is only an estimation, also the total system power density is remarkably higher. Comparison of total system specific power shows that the specific power of solution B is over five times as high as in solutions A and C which is partly explained by the lack of input filter's heavy smoothing reactors but still indicates that solution B is light in relation to its high output power.

3.3.3 Tolerance to environmental stresses

The tolerance to environmental stresses of the solutions are considered in Table 4. Ingress protection rating of the cabinet, maximum operating altitude, operating temperature and cooling method are presented in it. The ingress protection rating requirement of the converter is IP 65 so that it can be pressure washed. Even though it is unclear whether or not solution B requires additional enclosure and how solution C's enclosure is realized eventually, all manufacturers state that they can meet this requirement.

Table 4. Comparison of environmental properties.

	Solution A	Solution B	Solution C	Requirement
Environmental protection	IP 65	IP 67	IP 65	>IP 65
Maximum operating altitude at the rated power [m]	2000	4000	(1000)	> 2000
Operating temperature range [°C]	–20…+55	–40…+70	–20…+55	–20…+55
Cooling	Liquid + closed circulation	Liquid	Liquid	Liquid

Next, the maximum operating altitude for each system at the rated power is considered. Solution A can handle altitudes up to 2000 m, solution B up to 4000 m and solution C has not been defining altitude so it must be considered to be able to handle only altitudes up to

1000 m AMSL, after which correction factors for cooling, clearance and creepage distances, fuse dimensioning et cetera are required to be taken into consideration.

Operating temperature for the converter is required to be –20…+55 °C which all the solutions can fulfil. Solution B's operating temperature range extends from –40 to +70 °C but they have not defined in the released documentation what kind of cooling liquid mixing ratio and flow rate this requires. Even though the cooling systems of different solutions have some differences, like the internal heat exchanger in the solution A that other systems do not have, all the solutions utilize liquid cooling that can be added to machine's existing cooling system and thereby meet the requirement. However, the manufacturer of solution B has stated that their solution would benefit from having a more efficient cooling system with lower inlet temperature for the cooling liquid, as it would allow them to reduce the size of some of the components and slightly more power could be drawn from modules. In practice, this would require similar separate cooling system as the battery pack has to be built for the converter, which mitigates the benefit achieved from smaller converter modules to some degree.

3.3.4 Control system characteristics

In Table 5 the control systems are presented on a general level. Epiroc has let manufacturers have quite free hands with realization of the converter control and therefore each solution has taken slightly different approaches.

Table 5. Comparison of control system.

	Solution A	Solution B	Solution C	Requirement
Controller	Centralized	Distributed	Centralized/Distributed	NA
Control interface towards the vehicle	CAN SAE J1939, Isolated DI and DO	CAN SAE J1939, DI, DO	AI, AO, DI, DO, CAN SAE J1939	

Considering the latest concepts from each manufacturer, all solutions utilize both hard-wired and CAN-bus -based control interfaces. The difference is that solutions A and B rely on CAN messages to control the converter with some additional hard-wired signals whereas

solution C uses mostly hard-wired control and CAN messages only for informative purposes. Another difference is that solution A utilizes centralized control system in which one single controller handles all the control operations and solutions B and C have a distributed control system, in which each module is controlled individually. Solution C can be realized also with SIL2 rated controller which is something other manufacturers cannot provide.

3.3.5 Product maturity

In Table 6 the maturity of the solution is presented. The maturity of different parts of the design as well as the overall maturity of the solution are compared based on the interactions with each and available open-source data is presented.

Table 6. Comparison of the solution maturity.

	Solution A	Solution B	Solution C
Product maturity			
-Converter	Existing design	Existing/Modified design	Ready design
-Infeed circuit	New design	None	New concept
-Control interface	Modified design	Existing design	Existing concepts
-Mechanical	New design	Existing concept/New design	New concept
-Overall	Prototype/Pre-series	Prototype/Pre-series	Concept

Considering the maturity of the converter's electrical design solution A is the most finalised. Solution A uses an existing design whereas both solutions B and C need to have their existing designs modified or redesigned. Solution B utilizes the manufacturer's existing buck-boost converter design and an upscaled version of their earlier developed isolation stage. The buck-boost is already on the market and its updated second-generation version is coming to the market in Q1 2023 but the precise release time for the updated resonant converter is unknown. Solution C utilises manufacturer's existing full-bridge converter design and a newly designed buck-converter for this solution. The manufacturer has built and tested bench-top prototypes of each converter, so they have verified the design with which they are confident to meet all the set requirements.

What comes to the infeed circuit design the solution A is again the most finalized. They have earlier experience of such design and they have done simulations of the resonant circuit with data that includes OCS parameters. Solution B does not include an infeed circuit at all as they think it is not necessary and their converter can handle any kind of input voltage as required, so one must consider oneself if this part of the concept is immature or mature. Due to small size and weight of their converter solutions there however is more than enough space for it, if it proves to be needed later. Solution C has taken the infeed circuitry into consideration while designing their solution. They have done simulations of it and been able to identify and source suitable components for it.

The control interface for solution A is the most finalised one. Both hard-wired and CAN-bus interfaces with vehicle has been set and even the CAN dictionary has been defined. Solution A is practically ready to be implemented to the vehicle's control system. Solution B utilises the same combination of CAN-based and hard-wired control interface concept as their existing buck-boost converter, so its interface is basically set also. However, they have not specified the used CAN communication protocol in the provided documentation so some modifications or additions might be required. If the protocol proves to be different from machine's SAE J1939 either the converter must be updated to use the same protocol or else an additional communication gateway unit is required to translate the protocol. The control interface for solution C combines also hard-wired and CAN-based communication but the details have not been fixed yet.

The mechanical concept for the solution A can be considered to be ready. They have made a detailed design which includes the whole mechanical structure of the converter both internally and externally. It has been specially designed for MT42 Trolley, so it is ready to be manufactured and installed. Mechanical design has not been tested against shock and vibrations but only a finite element method (FEM) analysis has been made to prove the concept. The first assembled unit on the machine should be used to test the mechanical structure in a real environment. Solution B concept is under design and its basic design is to be started at the beginning of year 2023 and finalized by the end of February 2023, after which the mechanical basic design should be ready also. The manufacturer has earlier experience on the intended environment for which some of their earlier systems have also been designed, so the concept most likely will follow the well proven design. At this point, it has not been communicated if the mounting frame for the converter modules will be part

of their supply or if it is for Epiroc to design. The mechanical concept for solution C is the most unfinished one of the three and this is mostly due to the manufacturer not having sufficient mechanical engineering capabilities nor experience from the intended harsh environment. The manufacturer has prepared a very basic level sketch of the converter which is mostly to present how the converter modules could be fitted inside the cabinet. The mounting of the cabinet to the vehicle nor the modules to the cabinet have been considered. The mechanical concept for the modules is more advanced but it also has been prepared only on concept or very basic level.

The overall maturity of the solution A can be considered to be the most advanced one of the three. The design is ready, and the manufacturer has started the converter prototype testing in the beginning of the year 2023. The first unit could be sent for testing to Epiroc during Q1 2023. Solution B is the second most finalised one as a total system. The design is to be started at the beginning of Q1 2023 and the first unit could be sent to Epiroc for testing before the end of Q2 2023. Solution C is the most immature of the three mainly due to the state of its mechanical concept. The manufacturer believes that the first unit could be sent to Epiroc for testing after nine months after it has been ordered meaning at the end of Q3 – beginning of Q4 2023 if it were ordered right away.

3.3.6 Solution costs

Finally, the costs of different solutions are compared. Some of the costs are indications and changes to them are possible but they can be used however to compare the commercial aspect of the solutions.

The non-recurring engineering (NRE) costs of solution B are the highest of the three and the NRE costs of solutions A and C are approximately the same. However, there might be some additional NRE costs on solution B if it needs an input stage or mechanical housing and due to solution C’s unfinished status, it is unclear how much for example the mechanical design and manufacturing the cabinet itself when sourced on a third party will increase to the estimated NRE and unit costs.

The unit cost of solution B is the cheapest of the three at every break point of the price which are one, five and 15 sets. The unit cost of solution A is the second lowest at every break point and cost of the solution C is the most expensive.

When the NRE + unit costs are considered at different break points of first machine, first six machines and first 16 machines, the solution A is the cheapest of the three if only one machine is built. However, because solution B's unit cost is remarkably cheaper than others at every break point, already second machine built utilizing it would bring the total cost below the cost of solution A as seen in Appendix B.

At six machine break point which could be considered realistic amount of machines built during a few following years, the total cost of using solution A is 31.7% more expensive than using solution B and using solution C is 73.5% more expensive than using solution B. Based on this information the solution B would be the most feasible commercially even if the NRE or unit costs were slightly increased due to possible changes in the design.

4 Conclusions

In this final chapter the objectives of the thesis are reviewed, answers to research questions are summarised, and the results of the market study and the comparison are briefly discussed. Also, the importance and the novelty value of the thesis are evaluated, delimitations are stated, and future research topics are suggested.

4.1 Fulfilment of research objectives

The objective of this thesis was to compare different high-power DC-DC converter solutions to determine which one of those is the best fit for a full electrical NRMM application utilising a trolley solution as an external power source. Common step-down converter topologies, semiconductor switches and discrete components used in these converters as well as recent development in semiconductor switch technology were touched to understand how these converters are built and operated. Requirements for converter matching the application were set, a market study was conducted, and the results were compared against one another and the set requirements. During the market study a dozen of potential manufacturers specialised in converters for high power applications were found. Five of these were presented in the thesis and the three most promising ones were shown in the comparison. Comparison managed to point out the advantages and disadvantages of each solution based on which the most suitable solution for Epiroc could be decided.

4.2 Review and assessment of the findings

In the first chapter of this thesis two research questions were set the first one being how much better power density can be achieved in high-power DC-DC converters by using WBG semiconductor switches instead of Si-based switches. Based on limited sample size presented in this thesis far-reaching conclusions cannot be drawn. However, it can be stated that WBG semiconductor switches themselves do not reduce the volume of the converter but the increased switching frequency they enable has a remarkable effect on the volume of the converter as the size of the magnetic components can be reduced. In the case of converter

modules presented in this thesis the power density of converter modules utilizing WBG based semiconductors was 160 – 1400 % higher than the same of a solution utilizing traditional Si IGBTs.

The second research question set was to determine which one of the commercial solutions on the market suits best the needs of Epiroc. While each of the solutions have their strengths it can be concluded that solution B is the most suitable solution for a trolley application because it matches the set requirements and even exceeds most of them. It provides enough power to cover the whole machine portfolio with just two converter modules and its power density and specific power outmatches other solutions by far. It also has an advantage of being used in a similar environment on another NRMM already, so its mechanical design has been proven to withstand high shock and vibration levels typical to the application. The biggest question in its suitability is the input filter which is not part of the design but due to the small volume of the converter modules, there is room to add such an input filter later if such proves to be needed during testing. Solution B is also the cheapest long-term solution of the three. Solutions A and C were on par with each other on most of the studied aspects. Solution A's advantage was its matureness and solution C's its modularity and ability to output required power at full input voltage range. Disadvantages then again for both solution A and C were their large size and heavy mass, their relatively high cost especially long term and low power density and efficiency when compared to solution B.

Epiroc can base their decision of the used converter solution for the series produced MT42 Trolley with the aid of the findings presented in this thesis. The outcome of the comparison helps them to select a solution which is both technically and commercially suitable for them. Market study can be utilized also if such high-power converters are needed in any other machine as they are currently electrifying their machine portfolio or companies found in it may have other products which Epiroc could utilize.

In wider perspective the study conducted in this thesis is a small but vital part of the project which aims to reduce the carbon emissions caused by mining industry by electrifying the machine fleet and improving its usability beyond the level set by diesel-powered machines. As the literature study conducted in the beginning of this study shows, comparisons and market studies like this are rare or seldomly released for a public audience. So even though this thesis focuses only on presenting existing knowledge and anything new is not invented,

anyone interested about high-power DC-DC converters used in a challenging environment might find this study useful.

4.3 Comparison to earlier studies

As similar comparison of different high-power converter solutions was not found in the literature review, a direct comparison of the findings is not possible. However, comparison of similar topologies used in the solutions presented in this thesis were covered in study conducted by Steigerwald et al. (1996). Their comparison did not make any conclusions, but it suggested that the mass of the magnetic components for DAB converter was the lightest of the compared topologies and the efficiency of the auxiliar resonant commutated bridge (ARCB) converter's was the highest by a small margin. DAB topology was one of the topologies suggested also in other referred literature for such a high-power application but only one of the solutions found in the market study conducted for this thesis was utilizing it. Instead, most of the solutions found were constructed using two different cascaded converter topologies to meet all the requirements such as high voltage gain and the isolating structure as was suggested by Guo et al. (2020).

Suitability of different semiconductor technologies for such high-power DC-DC converter suggested by referred literature was also confirmed, as all the found solutions utilised either Si IGBTs or SiC MOSFETS but no solutions utilizing GaN technology for a such high voltage level application was not found.

4.4 Limitations of the study

Each of the three manufacturers whose solutions were compared in this thesis have given other proposals for alternative solutions or indications of such during the discussions, the latest of which was from manufacturer of solution B received during the finalization of the writing of this thesis. This solution is similar to the one described in this thesis, but it utilizes converter modules that exist already on the market so its NRE costs are lower, and the solution could be taken into use practically immediately. Manufacturers of solutions A and C also have suggested other proposals on how the solutions presented in this thesis could be improved. For example, solution A could be improved by designing a SiC MOSFET based

switching stages and solution C by redesigning the full-bridge converter so that the extra buck converter would not be needed. Both of these changes would have a positive effect on the size and volume of these systems. However, due to immature state of the proposal or receiving those so late, it was required to leave these alternative solutions out of this thesis.

Study does not take into consideration all the aspects of the converter design. Topics such as electromagnetic compatibility (EMC), input filter design, overload and short circuit protection, control logic of the solutions or switching methods and their effects on the voltage quality are not considered at all or have been discussed only superficially.

4.5 Research topics for the future

As electric vehicles are becoming more common, the market for these kinds of converters is also increasing. Hence, it can be expected that new solutions are brough to the market for example from manufacturers that were left out of the comparison or were found but not presented in this thesis. Therefore, in addition to comparing alternative solutions from the manufacturers of solutions A, B and C presented in this thesis in the near future, it would be also interesting to conduct a new market study after a few years to find new potential solutions or manufacturers.

Currently the SiC technology is the only one of the WBG technologies suitable and mature enough for this kind of an application. Research on a number of different semiconductor materials such as diamond are however ongoing to find new WBG technologies to further improve the characteristics of semiconductor switches. When these technologies are more mature and commercially available it would be interesting to see how converters built using those compare to ones found in this thesis. Development and maturing of SiC technology might also have interesting effects on converter technology in near future.

References

Alavi, P., Babaei, E., Mohseni, P. & Marzang, V. 2020. Study and analysis of a DC-DC soft-switched buck converter. IET power electronics, 2020. Vol.13 (7). p. 1456–1465

Andersson, A-S. 2021. Boliden collaborates with Epiroc and ABB on journey towards fossil free mine. Epiroc Newsroom. Accessed 25.2.2023. Available at: https://www.epiroc.com/en-uk/newsroom/2021/boliden-collaborates-with-epiroc-and-abb-on-journey-towards-fossil-free-mine

Ang, S. & Oliva, A. 2010. Power-switching converters, Third edition. Florida, Taylor & Francis group

Ballestín-Fuertes, J., Muñoz-Cruzado-Alba, J., Sanz-Osorio, J.F. & Laporta-Puyal, E. 2021. Role of wide bandgap materials in power electronics for smart grids applications. Electronics 2021, 10, 677, p. 1–26, Accessed 19.2.2023, Available at https://doi.org/10.3390/electronics10060677

Barbi, I. & Pöttker, F. 2018. Soft commutation isolated DC-DC converters. Springer Cham

Biela, J., Schweizer, M., Waffler, S. & Kolar, J. W. 2011. SiC versus Si – Evaluation of potentials for performance improvement of inverter and DC-DC converter systems by SiC power semiconductors. IEEE transactions on industrial electronics. Vol. 58. no. 7. July 2011. p. 2872–2882

Brown, M., Kularatna, N., Mack, R. A. Jr & Maniktala, S. 2008. Power sources and supplies world class designs, Elsevier Inc.

Climate watch. Historical GHG emissions. 2023. Wahington, DC: World resource institute. Accessed 25.2.2023, Available at https://www.climatewatchdata.org/ghg-emissions

Cruzat, J. V. & Valenzuela, M. A. 2018. Modelling and evaluation of benefits of trolley assist system for mining trucks. IEEE transactions on industry applications. Vol. 54. no. 4. July/August 2018. p. 3971–3981

Dimitrijev, S. 2012. Principles of semiconductor devices, Second edition. New York, Oxford University Press.

Erickson, R. W. & Maksimovic, D. 2020. Fundamentals of power electronics, Third edition. Springer Nature Switzerland AG

Fan, S., Pu, T., Liu, G., Ma, W., Li, L. & Williams, B. 2014. Current output hard-switched full-bridge DC/DC converter for wind energy conversion systems. IET Renewable power generation, 2014, Vol. 8, no. 7, p. 749–756

Guo, Z. & Sha, D. 2020. New topologies and modulation schemes for soft-switching isolated DC-DC converters. CPSS power electionics series. Singapore, Springer

He, P. & Khaligh, A. 2017. Comprehensive analyses and comparison of 1 kW isolated DC-DC converters for bidirectional EV charging systems. IEEE transaction on transportation Electrification. Vol. 3. no. 1. March 2017. p. 147–156

Kazimierczuk, M. K. 2016. Pulse-width modulated DC-DC power converters, Second edition. Chichester, John Wiley & Sons, Ltd

Koellner, W. G., Brown, G. M., Rodriguez, J., Pontt, J., Cortes, P. & Miranda, H. 2004. Recent advantages in mining haul trucks, IEEE transactions on industrial electronics. Vol. 51. no. 2. April 2004. p. 321–329

Lakkas, G. 2016. MOSFET power losses and how they affect power-supply efficiency. Texas Instruments analog applications journal (AAJ 1Q 2016). p. 22–26 Available at https://www.ti.com/lit/pdf/slyt664

Lindgren, L., Grauers, A., Ranggård, J. & Mäki, R. 2022. Drive-cycle simulations of battery-electric large haul trucks for open-pit mining with electric roads. Energies 2022. 15. 4871. p. 1–19. Available at https://doi.org/10.3390/en15134871

Lumbreras, D., Zaragoza, J., Mon, J., Galvez, E. & Collado, A. 2019. Efficiency analysis of wide band-gap semiconductors for two-level and three-level power converters. IECON 2019 – 45th annual conference of the IEEE industrial electronics society. 14th-17th October 2019. p. 1–7

Mack, R. A. 2005. Demystifying switching power supplies. Elsevier Inc.

Mazumdar, J., Koellner, W. & Moghe, R. 2010. Interface issues of mining haul trucks operating on trolley systems. 2010. Twenty-fifth annual IEEE applied power electronics conference and exposition (APEC). p. 1158–1165

Millan J., Godignon, P., Perpina, X., Perez-Tomas, A. & Rebollo, J. 2014. A survey of wide bandgap power semiconductor devices. IEEE transactions on power electronics. 2014. Vol. 29. no. 5. p. 2155–2163

Mohan, N., Undeland T. M. & Robbins, W. P. 1995. Power electronics – converters, applications, and design, Second edition. New York, John Wiley & sons, Inc.

Måård, M. 2022. Epiroc increases focus on sustainable mining with Smart and Green series. Epiroc Newsroom. Accessed 3.11.2022. Available at https://www.epiroc.com/en-fi/newsroom/2022/epiroc-increases-focus-on-sustainable-mining-with-smart-and-green-series

Nan, X. & Sullivan, C. R. 2009. An equivalent complex permeability model for litz-wire windings. IEEE transactions on industry applications. Vol 45. no 2. March/April 2009. p.854–860

Nayanasiri, D. & Yunwei, L. 2022. Step-down DC-DC converters: an overview and outlook. Electronics 2022, Vol. 11, p. 1693. Available at https://doi.org/10.3390/electronics11111693

Paraszczak, J., Svedlund, E., Fytas, K. & Laflamme, M. 2014. Electrification of loaders and trucks – A step towards more sustainable underground mining. International conference on renewable energies and power quality (ICREPQ'14). Cordoba (Spain). 8th-10th April 2014. Available at https://icrepq.com/icrepq'14/240.14-Paraszczak.pdf

Rachid, A., Fadil, H. E. & Giri, F. 2018. Dual stage CC-CV charge method for controlling DC-DC power converter in BEV charger. 2018 19th IEEE Mediterranean electrotechnical conference (MELECON). 2nd–7th May 2018. p. 74–79

Steigerwald, R., De Doncker, R. & Kheraluwala, M. 1996. A comparison of high-power DC-DC soft-switched converter topologies. IEEE transactions on industry application. 1996. Vol 32. no 5. p. 1139–1145

Swallow, T. 2021. ABB group partners with Epiroc to electrify mining processes. Mining digital. Accessed 4.3.2023. Available at https://miningdigital.com/technology/abb-group-partners-epiroc-electrify-mining-processes

Tamyurek, B. & Kirimer, B. 2015. An interleaved high-power flyback inverter for photovoltaic applications. IEEE transactions on power electronics. 2015. Vol. 30. no 6. p 3228 – 3241

Wang, F., Zhang, Z. & Jones, E. A. 2018. Characterization of wide bandgap power semiconductor devices. London, England: Institution of Engineering and Technology

Wintrich, A., Nicolai, U., Tursky, W. & Reimann, T. 2015. Application manual power semiconductors. SEMIKRON International GmbH. Available at https://www.semikron-danfoss.com/dl/service-support/downloads/download/semikron-application-manual-power-semiconductors-english-en-2015.pdf

Zhao, B., Song. Q., Liu, W. & Sun, Y. 2014. Overview of dual-active-bridge isolated bidirectional DC-DC converter for high-frequency-link power-conversion system. IEEE transactions on power electronics. 2014. Vol. 29. no. 8. p. 4091–4106